The impact of small-scale land cover and groundwater interactions on base flow solute and nutrient export in a small agricultural stream

Reid E. Buskirk · Jonathan M. Malzone ⬤ · Walter S. Borowski · John Cornelison

Abstract Central Kentucky could be considered a critical source area of nutrients in water ways because of low permeability soils, fast groundwater flow through bedrock fractures, and pervasive agriculture and development. Of particular concern is rising development in rural areas, which creates mixed land cover (MLC) watersheds, i.e., watersheds with development, agriculture, and other land cover types. MLC watersheds add complexity to spatial and temporal releases of dissolved constituents, leading to less predictable water quality patterns. The goal of this research was to examine the export of dissolved substances from a small, upland MLC catchment in central Kentucky with a focus on how the interaction between discharges from developed agricultural land cover and groundwater influence base flow water quality. Our approach was to spatially sample a representative catchment monthly over 1 year, characterize the major dissolved constituents, and evaluate catchment processes with statistical analyses and Piper diagrams. Principal component analysis, factor analysis, and Piper diagrams indicate base flow was composed of groundwater influenced by two different host rocks and an outfall draining a developed region.

Base flow nutrient export was dominated by mixing nitrate-sulfate rich groundwater with ammonium-phosphate-chloride rich outfall drainage. High nitrate groundwater dominated nitrogen export in the winter, whereas high ammonium outfall drainage dominated summer export. Spatial analysis revealed that ~ 10% of the basin may have similar land cover and hydrologic processes, suggesting that MLC catchments are small but collectively significant nitrogen sources to river networks due to development and agriculturally impacted groundwater.

Keywords Nutrient · Base flow · Principal component analysis · Factor analysis · Headwater catchment · Land cover · Mixed land cover watershed

R. E. Buskirk · J. M. Malzone (✉) · W. S. Borowski · J. Cornelison
Department of Geosciences, Eastern Kentucky University, 521 Lancaster Avenue, Richmond, KY 40475, USA
e-mail: jonathan.malzone@eku.edu

Introduction

Excess nutrient contamination released to water ways in the USA continues to be a concern for drinking water and aquatic ecosystems because it triggers eutrophication, which fosters the growth of toxic algal blooms, hypoxia in water bodies, and the loss of aquatic biodiversity (Dubrovsky et al. 2010; Jessen et al. 2015; Lopez et al. 2008). For example, non-point source nutrient export from agricultural, urban, and industrial landscapes has led to the creation of a hypoxic, or "dead zone" in the Gulf of Mexico associated with the outflow of the Mississippi River delta (Dubrovsky et al. 2010; Howarth 2008; HTF 2008; Turner et al. 2006; Turner et al. 2012). Given the increased intensity and amount of

rainfall predicted to occur from future climate change in the upper Mississippi basin, nutrient contamination of waterways, particularly from nitrogen, will likely increase and require reduction strategies that are difficult to meet without economic hardship (Sinha et al. 2017; Wu and Tanaka 2016). The scale and economic difficulties of nutrient reduction have led researchers to identify critical source areas (CSAs) that are prone to produce excessive nutrients per unit area of watershed, which allows effective prioritization of manageable clean-up targets (Ghebremichael et al. 2013; Giri et al. 2016; Qiu 2009). CSAs are generally classified as areas with a high likelihood to produce large amounts of runoff and sediment due to climate, slope, collection area, low soil permeability, agricultural or urban land cover, and high erosion potential (Giri et al. 2016; Huang et al. 2015). It has been found that CSAs can cover as little as 5% of a watershed's area, but yield as much as a fifth of total nutrient loads (White et al. 2009).

Central Kentucky can be considered a CSA due to the prevalence of low permeability soils, developed and agricultural land cover, and relatively fast groundwater flow due to fractures, bedding planes, and karst (Crain and Martin 2009; Currens and Graham 1993; Husic et al. 2017; Ray et al. 1994; Wolock et al. 2004). This region discharges into the Ohio River, which is responsible for approximately 41% of total nitrogen load from the Mississippi River system (HTF 2008). Central Kentucky likely contributes to this amount significantly, for example, the Kentucky River at Lock 2 has been measured to contribute $11,339 \pm 913$ metric tons of total nitrogen and 1088 ± 274 metric tons of total phosphorus (Crain and Martin 2009). Because higher order rivers, such as the Mississippi River, have been found to have low nutrient retention and act more as a nutrient conduit, current research suggests that nutrient reduction strategies should be targeted within headwaters where retention may occur (Gomi et al. 2002; Loken et al. 2018; Peterson et al. 2001). Nutrient reduction strategies in this region could lead to impactful improvement in water quality on small to large scales, but more data defining the timing and processes of nutrient loading from headwaters is needed in order to inform these efforts.

The role of groundwater on the spatiotemporal distribution of nutrient retention and export in small upland catchments has been underscored recently in addition to the controls of variable discharge and channel-sediment interactions (Bernal et al. 2015; Burrows et al. 2018; Siebers et al. 2016; von Schiller et al. 2017). Small

upland catchments have variable surface flows depending on climate, connection to groundwater, and geologic properties causing many to be intermittent or ephemeral with spatially heterogeneous hydrologic connectivity (Costigan et al. 2016; von Schiller et al. 2017). Nutrients such as dissolved phosphorous are correlated strongly with stream discharge during storm events that can account for over 70% of phosphorous export despite the fact that storm flow only occurs ~ 10% of the time due to the mobilization of sediment from channels, tile drains, and soils (Gentry et al. 2007; Pionke et al. 1999; Pionke et al. 1996; Royer et al. 2006). Despite the strong connection between nutrient export and rainfall-runoff relationships, groundwater can contribute to the nutrient export in small upland catchments as a result of both seasonal fluctuations in regional gradient and transient activation of shallow perched systems (Zimmer and McGlynn 2017, 2018). Longitudinal trends in nutrient concentration along streams can be a result of dynamic groundwater-surface water interaction and in-stream processes, where groundwater often controls nutrient transport during dry periods by sustaining overland flows, adding nutrients, diluting surface water nutrient loads, and contributing carbon (Bernal et al. 2015; Burrows et al. 2018). Nitrogen export from upland watersheds has been shown to be sensitive to groundwater patterns such as seasonal seep dynamics, riparian residence times, and lithology (Butturini et al. 2003; O'Driscoll and DeWalle 2010; Valett et al. 1996). Agricultural nitrogen in shallow groundwaters has made base flow a potentially dominant mechanism for nitrogen export, where base flow periods can account for ~ 60% of nitrate export (Burow et al. 2010; Pionke et al. 1996). Understanding how groundwater with elevated nutrients controls base flow exports in small upland catchments could help to focus ongoing nutrient management issues in central Kentucky (McAlister et al. 2010; Carey et al. 1994; Kentucky River Watershed Watch 2010, 2011, 2012, 2013, 2014, 2015, 2016, 2017).

For mixed land cover (MLC) catchments, the addition of anthropogenic point and non-point sources along with complex groundwater and runoff processes makes it difficult to identify critical nutrient sources as a number of processes combine to produce the overall nutrient export signal (Coulter et al. 2004; Lee et al. 2016). Agricultural land cover often may account for the majority of nutrient export due to agrochemical use, animal husbandry, farm practices, and tile drainage, which add large amounts of nitrogen, phosphorous, and sediment

to water ways (Brisbois et al. 2008; Ford et al. 2018; Nguyen et al. 1998; Vadas et al. 2015; Withers and Hodgkinson 2009). Developed land cover also contributes significant levels of nutrients and sediments via deposition from vehicles, household and lawn operations, construction activities, discharges from pipes and gutters, and sewage effluents (Fork et al. 2018; Hobbie et al. 2017; Lee et al. 2016). When agricultural and developed land covers are combined in MLC catchments, the impact of nutrients in water ways becomes exacerbated. Specifically, the continuous nutrient contributions from agriculture overloads the stream retention capacity and episodic runoff events from developed land cover increase nutrient levels further and reduce the lag time between pollution source emissions and peak stream concentration (Chen et al. 2018). Additionally, the loading of streams with nutrients and contaminants in MLC watersheds can be spatiotemporally dynamic given the distribution patterns in anthropogenic land cover and stream flow dynamics, where variable source/sink and dilution processes can lead to unexpectedly patchy distributions of pollution (Hubbart et al. 2017; Shi et al. 2017). The threshold for such impacts from development added to mixed catchments is low, where coverages of less than 1% of catchment area can lead to detectable water quality changes (Mehaffey et al. 2005). Because MLC watersheds in Kentucky export 34% more total P and 53% more total N compared with undeveloped watersheds (Crain and Martin 2009), nutrient reduction in this region could be achieved by identifying sensitive regions in watersheds in order to prioritize development in locations where impacts are likely to be less severe (Martin-Mikle et al. 2015).

The overarching goal of this research was to examine the seasonal nutrient export of a small MLC upland catchment in central Kentucky with an emphasis on how the interaction between discharge from developed agricultural land cover and groundwater leads to base flow export of dissolved constituents. The approach was to spatially and temporally sample a small-scale representative catchment that (1) contained mixed developed and agricultural land covers; (2) was not classified as a first-order stream or higher; and (3) directly discharged to a higher order stream. This approach was chosen because it was suspected that these regions were sensitive, critical source areas of nutrients due to the spatial coverage of this type of catchment, the occurrence of thin low permeability soils, and the well-developed channels that quickly export water past the riparian zone

of larger order streams. The aim of quantifying this small-scale system was to better understand how nutrients may be managed in the region and to provide primary data to inform the selection of targeted management practices.

Methods

Site description

Sampling sites were located in a small, intermittent, MLC catchment ($0.5 km^2$) that feeds into the Muddy Creek watershed in east-central Kentucky (Fig. 1). The Muddy Creek watershed is a 4th order basin ($176 km^2$) that ultimately feeds into the Kentucky River, part of the Ohio and Mississippi drainage systems. This region lies in the eastern portion of the Kentucky Bluegrass, characterized by rolling hills, interbedded limestone and shale bedrock, and average yearly rainfall of 1100 mm and average yearly temperature of 13 °C (NRCS 2006). The hydrologic landscape region (HLR) for this area was classified as either low permeability soil with permeable bedrock or low permeability soil with low permeability bedrock (Wolock et al. 2004). In these HLRs, the low permeability of soil leads to higher amounts of runoff with a patchy distribution of springs where permeable bedrock occurs. As typical of streams draining agricultural and developed lands, the Muddy Creek watershed exhibits NO_3^- loading and elevated *Escherichia coli* levels (McAlister et al. 2010; LaSage et al. 2006; Kentucky River Watershed Watch 2010, 2011, 2012, 2013, 2014, 2015, 2016, 2017).

As predicted by the local HLR, the field site contains thin (< 1 m), low permeable clay silt to silty loam soils. Two major drainage channels flow from west to east and north to south in the catchment and meet up at the outlet facing southeast (Figs. 1 and 2a). The channels generally lack riparian zones and were steeply incised in some locations by 1–2 m. Land cover consisted of cattle pasture and cultivated crops with some developed regions (Fig. 2b). Developed areas mainly consisted of roads, a dairy complex, a swine barn, office facilities, farm vehicle facilities, and storage silos. The catchment's underlying bedrock consisted of the Crab Orchard Formation, Boyle Dolomite, and New Albany Shale (Fig. 2c; Greene 1968; KGS 2020). An expanded regional geologic map shows the relationship of the site to the surrounding area (Supplemental Figure 1). These
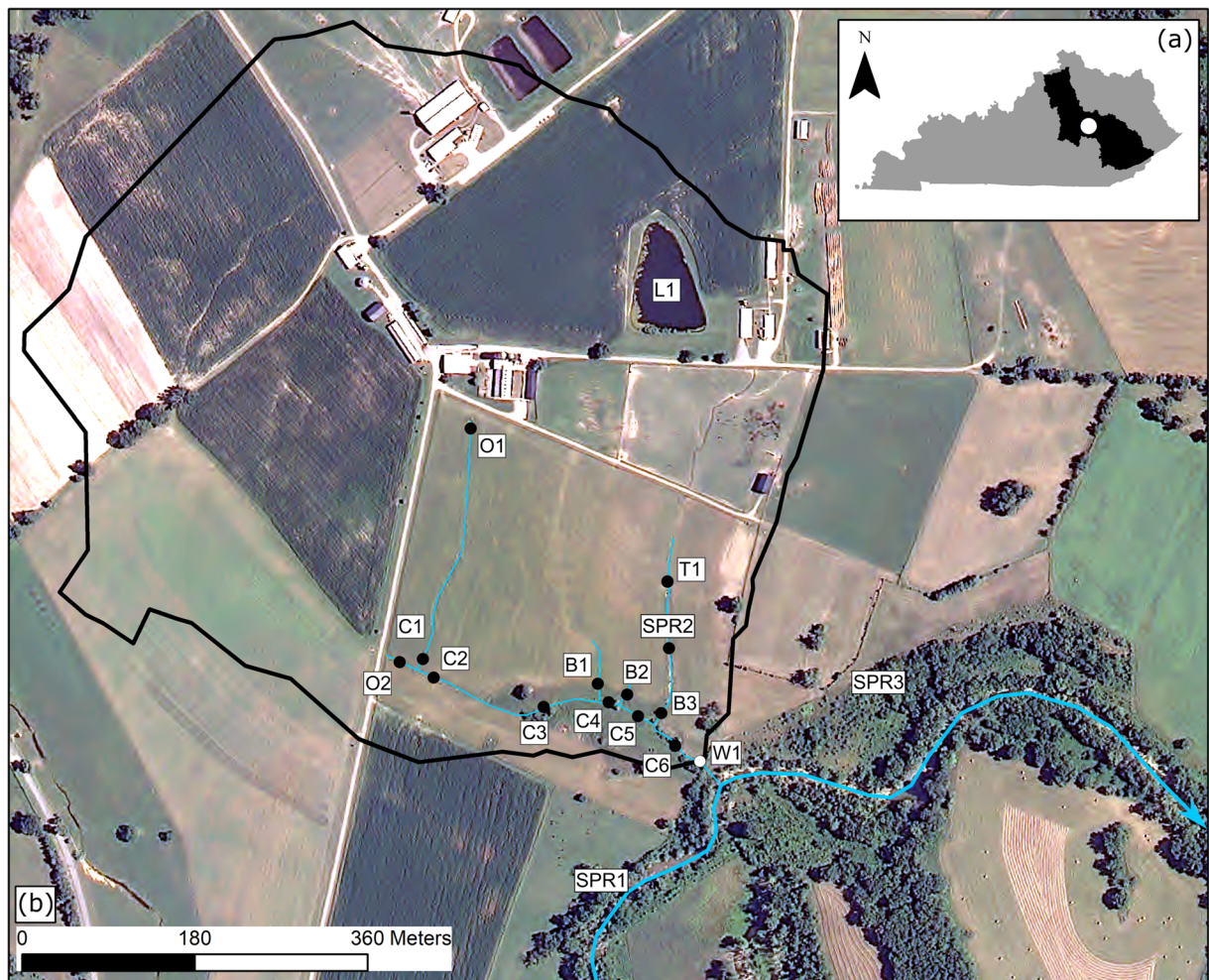
Fig. 1 (**a**) Inset map of Kentucky with the Kentucky River watershed shaded black and the study site marked with a white point (coordinates of W1: 37.718202, − 84.151826). (**b**) The research watershed (black outline) showing sampling stations (black dots) at outfalls (O), tiles (T), springs (SPR), open water (L), stream channels (C), and tributaries (B). Muddy Creek is outlined in blue and flows towards the east in this map as indicated by the arrow. The channels are highlighted in blue. The white dot represents the watershed outlet (W1)

units were a mixture of shale, limestone, and dolostone. The majority of the watershed, including the upland areas, was immediately underlain by the New Albany Shale (Fig. 2c). The contact between this unit and the underlying Boyle Dolomite was a generally impermeable clay unit that often caused groundwater to discharge at the boundary between these two units, forming springs (Supplemental Figure 2).

Sampling

The sampling sites for the MLC catchment in this study were chosen to account for different land uses and water types in order to observe their impact on water chemistry in resultant in-channel mixtures. These included major springs, outfalls, confluences, tile drains, and the watershed outlet (Figs. 1b and 2b). Springs represented groundwater sources into the catchment or were immediately outside the catchment (Fig. 1b). Springs outside the catchment were sampled to assess local variability in spring chemistry and to observe if inter-watershed connections could exist in the subsurface. Groundwater springs were identified by sight and confirmed with temperature measurements. Outfalls included point sources where pipe discharges fed into the main channel. These included a culvert draining from the developed region of the catchment into the main channel (O1), the outlet of a tile-drained agricultural

Fig. 2 (a) Digital elevation model of the research site with 5 m contours. (b) Land cover map for the study site with legend below. (c) Geologic map of the research site showing the extent of the Crab Orchard Shale (Scb), Boyle Dolomite (Db), and New Albany Shale (MDna). Map after Greene (1968); see Supplemental Figure 1 for geologic map of the lower Muddy Creek watershed
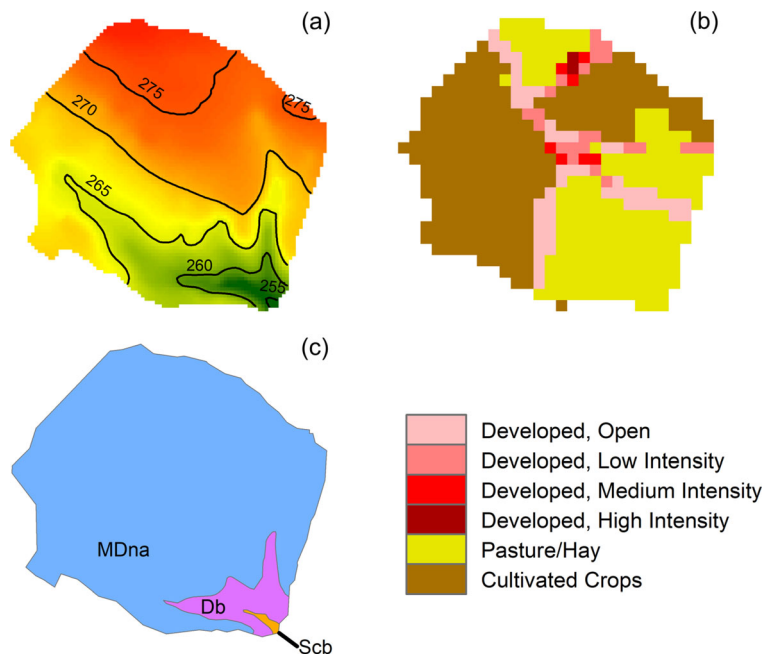
field located underneath a road into the main channel (O2), and a smaller tile drain outlet in a pasture field (T1). Characteristic reaches included sampling sites following the main drainage channel with regular sampling intervals along the stream and confluences (Fig. 1b). A man-made pond inside the watershed (L1), isolated from the main channel system, was also sampled for comparison to channel waters.

The main channel of the watershed begins at O1, courses to O2, then onward to C1, C2, and C3 through C6 until arriving at W1 and emptying into Muddy Creek. The main channel is joined by several tributaries. B1 is the first tributary joining the main channel just upstream of C4. The second tributary at B2 connects with the main channel upstream of C5. The most easterly tributary joins the main channel upstream of C6. Sampling sites T1, SPR 2, and B3 are situated on the same tributary channel (Fig. 1).

Collection of water samples from the sites occurred monthly between May 2017 and September 2018, usually on fair days with little or no storm-water flow. In the field, sampling sites were analyzed for pH, temperature, and electrical conductivity (EC) with a YSI ProDSS probe, calibrated before every sampling day. Water samples were directly collected with 60-ml syringes and filtered through a 0.45 μm filter. Samples were then stored on ice in a cooler for no longer than 8 h and then

transferred to a refrigerator until analysis, which occurred within 1 or 2 days for dissolved nutrients.

Chemical analyses

Dissolved major ions (chloride, Cl^-; sulfate, SO_4^{2-}; sodium, Na^+; potassium, K^+; calcium, Ca^{2+}; and magnesium, Mg^{2+}) were measured via ion chromatography using a Metrohm 930 Compact IC Flex system (Metrohm 2020; EPA 2007). Dissolved nutrients were measured via UV-Vis spectrophotometry using a Thermo Scientific Evolution 201 UV-Visible Spectrophotometer. Nitrate (NO_3^-) was measured using NitraVer5 powder packets (Hach 1997), based on the cadmium reduction method (Eaton et al. 2005b). Ammonium (NH_4^+) was measured via the phenol hypochlorite method (Eaton et al. 2005a as modified by Gieskes et al. 1991). Phosphate (PO_4^{3-}) was measured via the ascorbic acid method (Eaton et al. 2005c as modified by Gieskes et al. 1991).

Multivariate analyses

Principal component analysis (PCA) and exploratory factor analysis (FA) were performed on the resulting water sample dataset to identify data patterns that describe how different water sources affect main channel water chemistry. PCA and FA are widely used tools in

water quality studies to understand hydrological/geochemical processes in watersheds (Inamdar et al. 2012; Le et al. 2017; Lee et al. 2016; Love et al. 2004; Olsen et al. 2012; Pejman et al. 2009). These statistical methods reduce the dimensionality of datasets with many variables to produce principal components (PCs) and factors. Principal components are uncorrelated variables that capture the majority of dataset variance, whereas factors are latent variables that capture correlations among observed variables (Everitt and Hothorn 2011). Given an adequate set of variables, the PCs and factors should reflect natural processes behind chemical evolution of water originating from different hydrological compartments such as groundwater or tile drains. In order to reconcile PCA and FA results with the original data as an accuracy check, background spatiotemporal trends were analyzed independently prior statistical analysis to improve interpretation (Olsen et al. 2012; Le et al. 2017).

PCA was performed using the FactoMineR package in R on the correlation matrix of 190 individual samples from August 2017 to August 2018 using nine variables (Ca^{2+}, Mg^{2+}, Na^+, K^+, Cl^-, SO_4^{2-}, NO_3^-, NH_4^+, and PO_4^{3}) (Lê et al. 2008). Concentration values below detection limits were assigned as 0.0 values in the dataset. Data from May 2018 was excluded from the PCA because anion data (Cl^- and SO_4^{2-}) was not measured. PCA loading plots and bi-plot graphics were generated via the FactoExtra package in R (Kassambara and Mundt 2017).

FA was performed using the factanal() function of the core R program on the same raw matrix of 190 individual samples from August 2017 to August 2018 described above (Everitt and Hothorn 2011; R Core Team 2019). The number of optimal factors that best describes the data was determined using the nFactors package in R (Raiche and Magis 2020). Factors were considered significant if their eigenvalue was close to or greater than 1 (Love et al. 2004).

PHREEQC and Piper diagrams

Piper diagrams were constructed in order to characterize geochemical end members based on major ion composition that could be compared with statistical results (Appelo and Postma 2004). In order to construct Piper diagrams, alkalinity data were required. The bicarbonate ion concentration was not measured as part of the ion chromatography suite, because the method utilized a bicarbonate/carbonate eluent. Instead, bicarbonate/alkalinity was measured with a Hach digital titration method for select samples to determine normal ranges at the field site (Hach 2013). Because bicarbonate was determined to be the dominant anion by one to three orders of magnitude across the field site, the bicarbonate concentration was estimated for all samples using PHREEQC (Parkhurst and Appelo 2013). Each sample was simulated as a solution in PHREEQC using all observed parameters as inputs. Bicarbonate was added until the charge balance percent error of each solution fell below 1%. These solution outputs were taken as reasonable estimations given that bicarbonate was shown to be the dominant anion and that simulated values fell within observed ranges. An average concentration of major anions and cations was calculated for each site and plotted on Piper diagrams using the hydrogeo package in R (English 2017). Finally, a simple mixing model was conducted between identified end members using the mix function in PHREEQC in order to examine if channel water chemistry followed a simple mixing pathway.

Regional spatial analysis

In order to explore the possible impacts of small-scale processes on larger scale systems, spatial analysis was conducted to quantify the occurrence and land cover of watersheds similar to this study's in the local 4th order basin of Muddy Creek. Similar catchments were identified in the watershed by delineating all catchments that met the following criteria: the valley was not classified as a first-order stream or higher, the valley contained a well-developed channel, and the outlet directly discharged to Muddy Creek without first passing through a first-order stream. Valleys with well-developed channels were identified along Muddy Creek using the Kentucky State Single Zone Digital Elevation Model (KGN 2018). First-order and higher stream valleys were then subtracted from these data using the National Hydrography Flowline data, which maps perennial streams (Strahler 1957; USGS 2002). The coverage of the remaining valleys was delineated by using the hydrology toolbox in ArcGIS, which uses DEM data to calculate watershed coverages from user-specified outlets (ESRI 2018). The total coverage of watersheds that met these criteria were then compared to the total watershed area. Additionally, the land cover of these catchments was quantified and compared to the land

cover distribution of the whole Muddy Creek watershed. Land cover was quantified by extracting the Muddy Creek watershed area and similar catchment coverages from the 2011 National Land Cover Dataset (USGS 2014). The distribution of land cover between the 4th order basin and similar catchments as well as the distribution between all similar catchments were compared.

Results

Dissolved salts, nutrients, and physiochemical parameters

Major cations varied dependent on their source water (Fig. 3a–d). Sampling site O1 was a major base flow source of Ca^{2+}, Mg^{2+}, and K^+. Sites C1–C6 and W1 lie along the main channel originating near site O1 and show a declining average concentration of these cations moving downstream. The outlet of the watershed (W1) had elevated levels of these cations compared with sites not connected to O1. Springs and the tile drain showed relatively lower concentrations of Ca^{2+} and Mg^{2+}, although variation in Mg^{2+} tended to be greater. Tributary sites (B1, B2) and the man-made lake (L1) had the lowest concentrations of Ca^{2+} and Mg^{2+}, again with more variation in Mg^{2+}. Na^+ tended to have low variation at all sites, but O1 still had the highest average concentration. There was no clear dilution pattern moving downstream for Na^+ with only B2 showing relatively low concentrations. K^+ had a spatial concentration pattern similar to Ca^{2+} and Mg^{2+}; however, groundwater and tributary sites tended to have extremely low concentrations. Only the sites O1 and O2 appeared to behave as sources of K^+ that were then detected downstream and exported at the outlet W1.

The anions Cl^- and SO_4^{2-} had nearly opposite spatial distribution with respect to each other, but both were elevated at the watershed outlet (W1). Concentrations of Cl^- were similar to cation distributions, with O1 as the major source, and downstream sites exhibited progressively lower Cl^- concentrations (Fig. 3e). Site O2 also sometimes had higher levels of Cl^-. Conversely, SO_4^{2-} tended to increase downstream with the highest concentration observed at tributary sites (Fig. 3f). The main channel begins to show increasing amounts of SO_4^{2-} after the confluence with B1. Site W1 had Cl^- levels that were elevated relative to tributary sites and SO_4^{2-} levels

that were elevated relative to O1, indicating that both sources were important in the chemistry of water exported from the catchment.

Dissolved PO_4^{3-} and NH_4^+ had comparably similar spatial patterns to cations and chloride, whereas NO_3^- had higher concentration in groundwater and tile sources (Fig. 3g–i). O1 and O2 had the highest base flow PO_4^{3-} and were diluted in downstream stations (C1–C6). One difference PO_4^{3-} displayed from this pattern, however, was that the watershed outlet (W1) had relatively low levels. Even a large outlier of PO_4^{3-} concentration observed at O1 and O2 did not elevate W1 levels much. PO_4^{3-} was also elevated on one occasion in SPR 1. NH_4^+ concentrations were highest at O1 and elevated at W1 compared with tributary sites. The concentration of NH_4^+ was clearly elevated at O1 relative to other nutrients. There also was one occasion when NH_4^+ was high at SPR 1, showing the highest concentration in all spring water samples. Outside the study watershed, SPR 3 had the highest and most variable NO_3^- concentrations. Sites T1 and SPR 2 have the highest NO_3^- concentrations of sites connected to W1 and generally the outlet had elevated levels compared with the main channel and B1–B2.

General water physiochemical measurements (EC, pH, temperature) exhibited differences between outfalls, surface water, and groundwater (Fig. 3j–l). Typically, outfalls (O1 and O2) had high electrical conductivity, showing that they were the primary sources of dissolved ions (Fig. 3j). Dissolved ions decreased in-channel waters moving downstream. Springs, tributary sites, and T1 had lower pH values (closer to 7) than other water sources, while L1 had relatively high pH values > 8 (Fig. 3k). Temperature values indicated that groundwater had lower yearly variation in temperature than surface water (Fig. 3l).

Monthly observations demonstrated that the water characteristics of sampling sites at base flow have seasonal and other temporal patterns that impact the watershed outlet W1 (Fig. 4). The outfall O1 had a strong seasonal pattern with dissolved ions (EC, Ca^{2+}, Mg^{2+}, K^+, Cl^-, and NH_4^+). These dissolved ions increased to a maximum that was several times larger than background concentrations around September and October 2017 and gradually decreased to lower levels in the spring and early summer of 2018. W1 was influenced by these high concentrations in the upper watershed, having higher concentrations during this same time period. Na^+ was also generally highest at O1, but the overall trend during
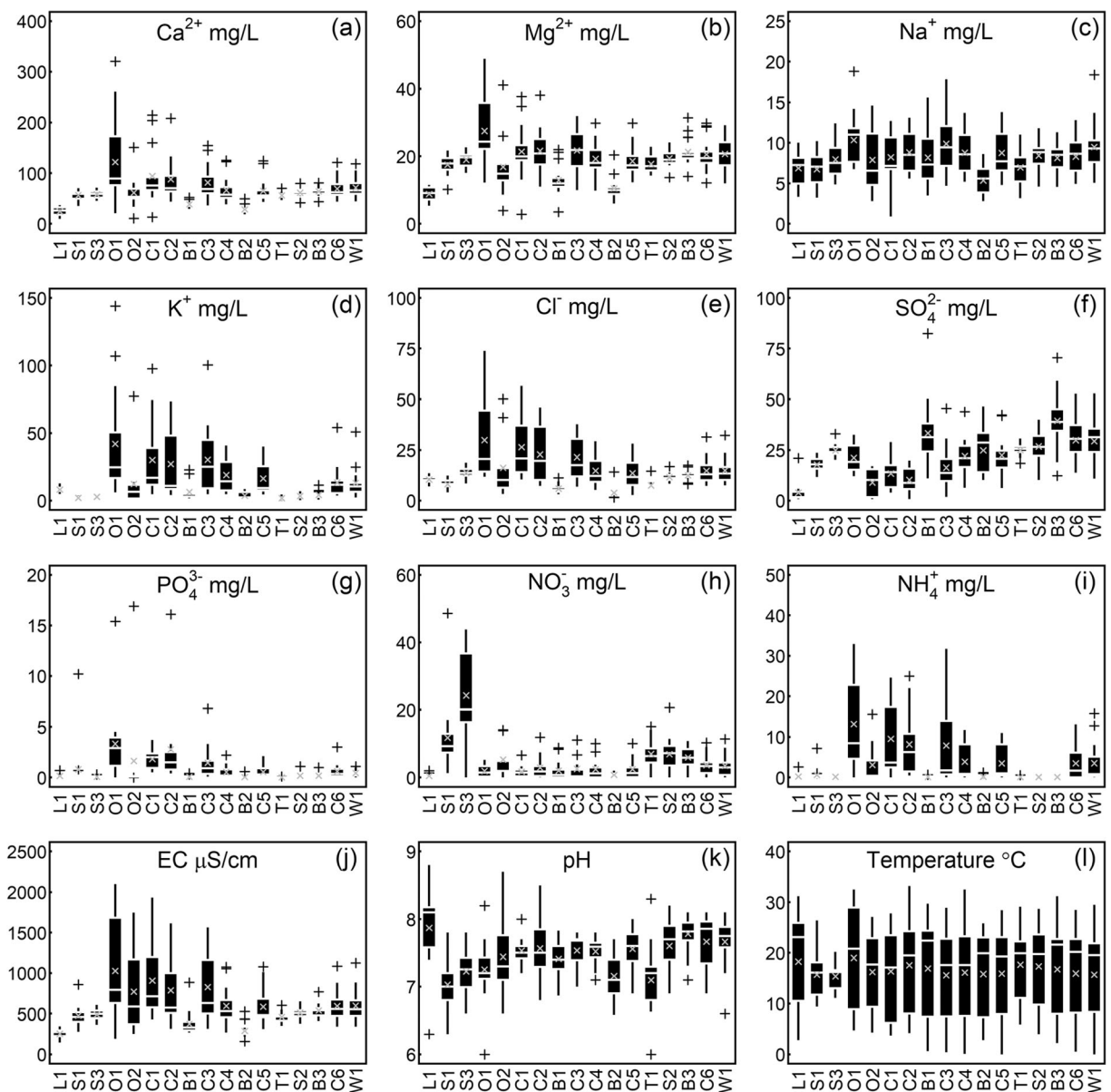
Fig. 3 Box and whisker plots showing statistics of the twelve measured parameters at each sampling site. Arithmetic mean (gray X's) and median (gray lines) values are shown within black boxes bounded by the 25th and 75th percentile values; lines extend to the 10th and 90th percentile values with outliers shown by crosses (+). Concentration units for solutes are in milligrams per liter (mg/L) with electrical conductivity (EC) in units of micro-Siemens per centimeter (μS/cm). Sites are listed as generally progressing down channel to the watershed outflow (W1)

the sampling interval was a slight decrease. SO_4^{2-} had a more variable pattern with the highest concentrations at sites influenced by groundwater contributions, especially during the latter part of 2017. The variable pattern in SO_4^{2-} at these sites was reflected in higher relative concentrations at the watershed outlet W1. PO_4^{3-} concentrations were generally lowest in August, and

remained below approximately 2 mg/L at B3, W1, and within groundwater. PO_4^{3-} concentration was typically elevated at O1 under base flow conditions but spiked to about 15 mg/L on one occasion in January 2017, likely due to a recent storm event. NO_3^- concentrations were highest in groundwater and at B3 and T1. Spring parameters did not show a seasonal pattern, yet were
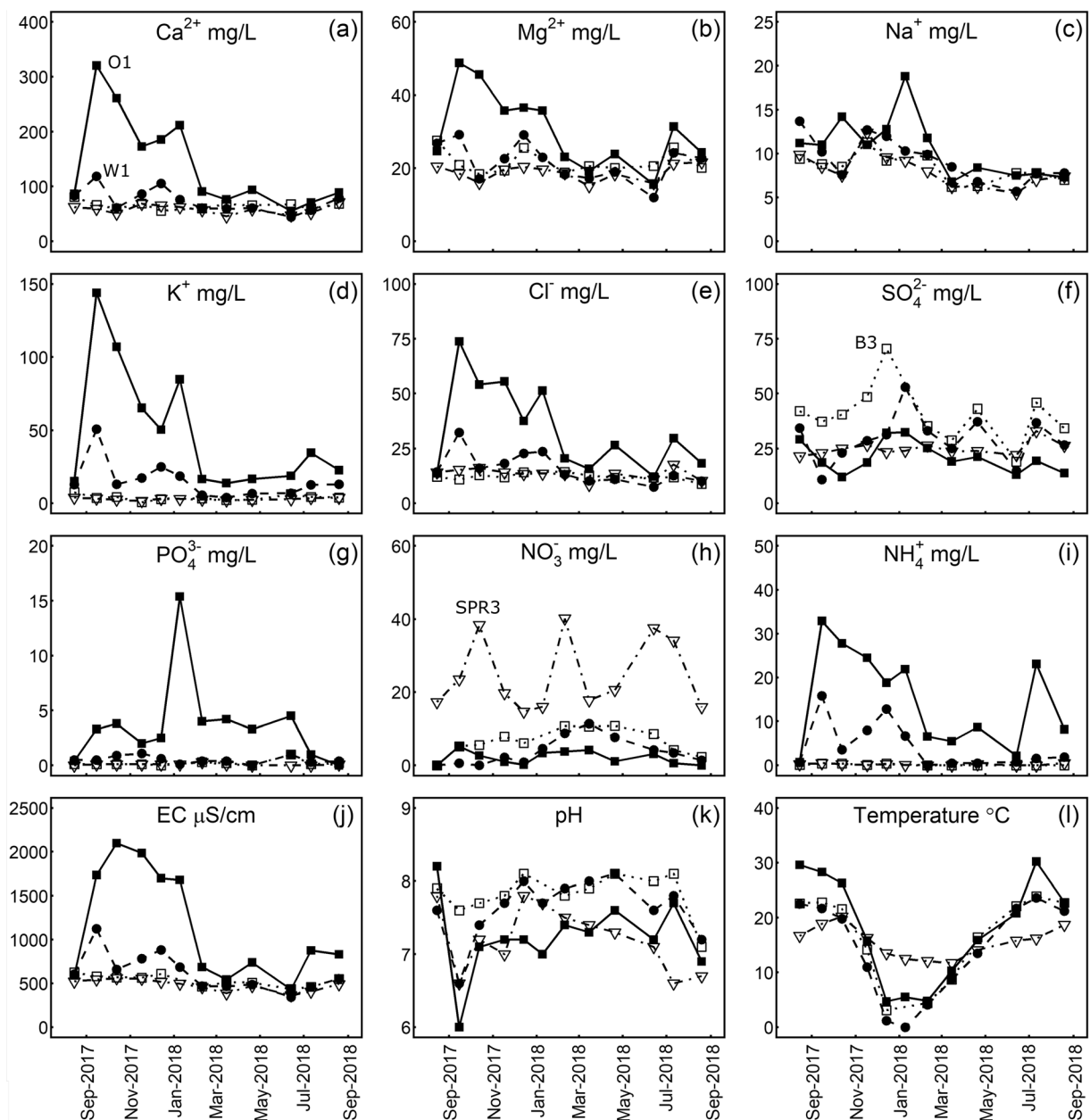
Fig. 4 Time plots of twelve measured parameters at O1 (black squares), SPR 3 (white triangles), W1 (black circles), and B3 (white squares) from August 2017 to August 2018

variable over the sampling period. Sites T1 and B3 exhibited seasonal NO_3^- increases in the winter and decreases in the summer. This seasonal pattern was also observed at W1 where NO_3^- concentrations peak in March and NH_4^+ peaks in the summer due to discharge from O1 (Fig. 5a). PO_4^{3-} at W1 did not show a clear seasonal pattern when compared with nitrogen (Fig. 5b).

Multivariate analyses

PCA identified three principal components (PCs) greater than the average PC percentage, capturing 82.9% of total dataset variation (Fig. 6a). PC1, PC2, and PC3 captured 57.4%, 14.8%, and 10.5% of dataset variation, respectively (Fig. 6a). Higher PC variable loadings

Fig. 5 (a) Column plots of N-NH$_4^+$, N-NO$_3^-$, and (b) P-PO$_4^{3-}$ concentrations in milligrams per liter (mg/L) at site W1 during the sampling period, which indicated nutrient levels exported from the study site over time
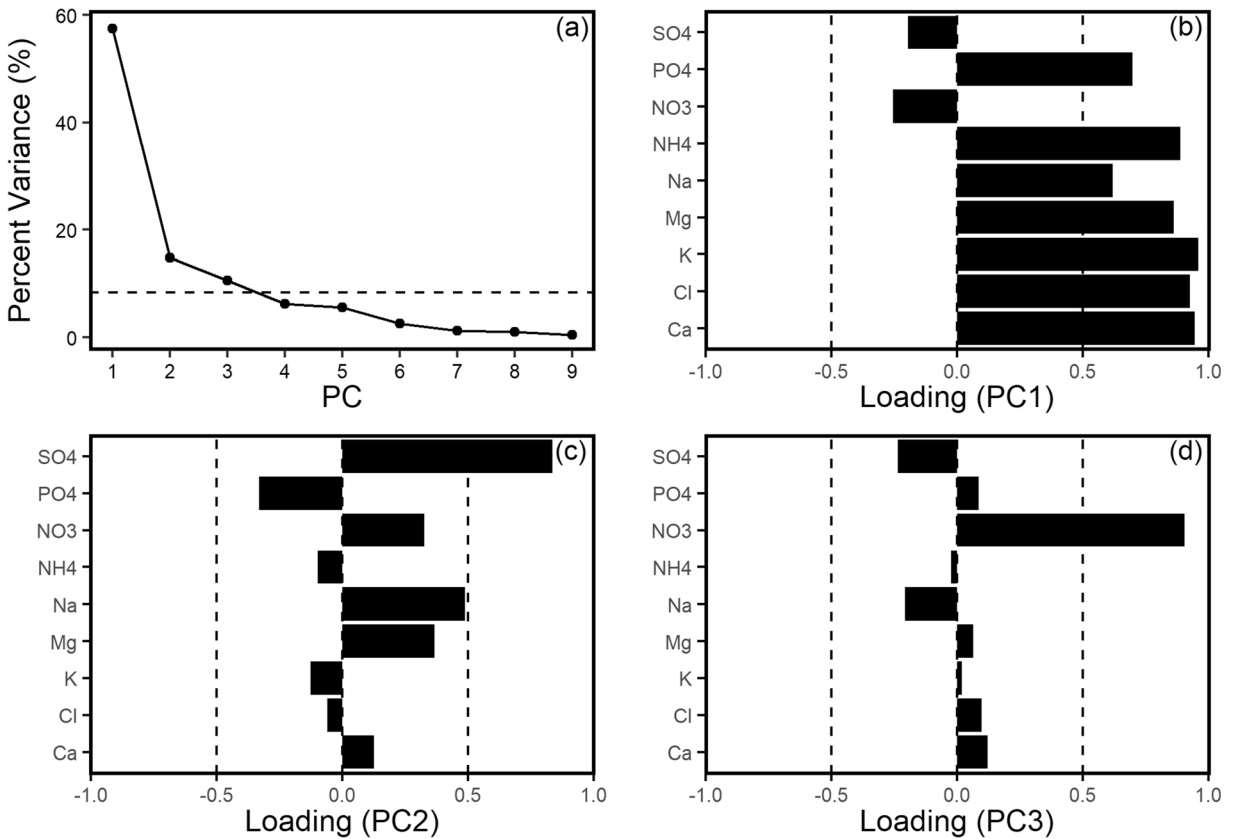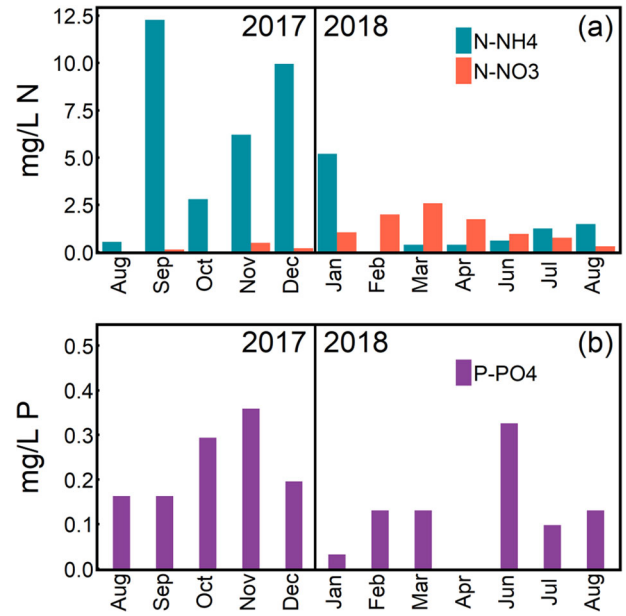
Fig. 6 (a) Scree plot of resulting principal components (PCs). The horizontal line shows the mean percent variance, which was used to select the first three principal components for interpretation.

Variable loading plots for (b) PC1, (c) PC2, and (d) PC3. The x-axis of these plots shows the direction and strength of parameter correlation

indicate greater variance captured by the PC. Hence, resulting PC loading significance was evaluated by considering loadings from 1 > 0.75, 0.75–0.50, and 0.50–0.30 as "strong," "moderate," and "weak," respectively, following the classification by Liu et al. (2003) for interpretation. PC1 had a strong and positive correlation with parameters Ca^{2+}, Mg^{2+}, K^+, Cl^-, and NH_4^+, as well as a moderate correlation for parameters Na^+ and PO_4^{3-} (Fig. 6b). PC2 was strongly and positively correlated with SO_4^{2-} (Fig. 6c). PC3 was strongly and positively correlated with NO_3^- (Fig. 6d).

A PC score plot for all sources of water indicated samples from O1 and the main channel typically ranged from large, positive PC1 scores to large, negative PC1 scores (Fig. 7a). The largest PC1 scores occurred at O1. Main channel samples formed a similarly shaped cluster to O1, but often exhibited lower PC1 scores. W1 had a smaller range of PC1 values compared with the main channel sites. Overall, these three groups exhibited the largest scores on September 2017. The lowest PC1 score for main channel and W1 samples overlapped with the tight, negative score ranges exhibited by contributing tributaries (sites B1, B2, B3), local springs (SPR 1, SPR 2, SPR 3), and the farm pond (L1).

Groundwater exhibited a tight PC2 range with most samples having positive scores (Fig. 7a). Tributaries showed a more variable PC2 cluster, which surrounded the groundwater cluster. The farm pond had a tight, negative PC2 cluster. Tributaries, groundwater, and W1 have similar PC2 score ranges. Main channel PC2 scores were similar to W1 scores, but some samples exhibited negative PC2 scores below the range of the farm pond sample cluster. PC2 ranges at W1 fell between the tributary and main channel scores.

Tributaries formed a tight cluster of PC3 scores along the PC1 axis, separate from the groundwater cluster (Fig. 7b). The farm pond cluster had the tightest cluster of PC3 scores about the PC1 axis, within the tributary group. The groundwater cluster had the highest PC3 scores and partially overlapped with the W1 cluster. Tributaries and W1 had similar PC3 ranges, but proximal sites within the main channel and O1 samples exhibited greater PC3 score ranges. Groundwater, tributary, main channel, and W1 clusters primarily intersected along the negative PC1 axis.

Simplified PCA plots showed a gradational axis between tributaries, groundwater, and O1 for PC1 with W1 samples clustering between these groups (Fig. 7c–d). Tributary B3 scores are more similar to groundwater

samples compared with sites B1–B2 (Fig. 7c–d). Along the PC1 axis, W1 typically had the lowest scores during the winter months, and the highest PC1 scores occurred during September 2017 (Fig. 7e–f). The lowest W1 PC1 scores plotted within the groundwater cluster from February–June 2018 (Fig. 7e–f). W1 samples plotted within the O1 sample cluster during September 2017 and for several months throughout the fall. W1 had a negative PC2 score during September 2017 (Fig. 7e). After this time, the remainder of the sampling campaign showed a generally counterclockwise movement of W1 PC1 and PC2 scores around the origin (Fig. 7e). For PC3, W1 had negative PC3 scores within the range of the tributary cluster most of the time, remaining relatively constant over the duration of the sampling year (Fig. 7f). W1 exhibits the highest PC3 scores in the spring, with the lowest score in January 2018.

Three factors were identified for FA each having an eigenvalue close to 1 or greater (Table 1). These three factors capture 68.5% of the total dataset variation with factors 1, 2, and 3 (F1, F2, F3) capturing 44.3%, 12.6%, and 11.6% of dataset variation, respectively (Table 1). F1 had a strong positive correlation with Ca^{2+}, Mg^{2+}, and K^+, as well as a moderate correlation with Cl^-, NH_4^+, Na^+, and PO_4^{3-}. F2 had a moderate positive correlation with Cl^-, NH_4^+, and Na^+, as well as a negative correlation with NO_3^-. F3 had a moderate positive correlation with PO_4^{3-} and a negative correlation with SO_4^{2-} (Table 1).

F1 has a comparable pattern to PC1, showing the largest positive values for O1 and channel sites connected to O1 and smaller negative values for tributary and groundwater samples (Fig. 8a). Generally, O1 has the highest F1 scores and the largest range, while channel water was related the O1 distribution with lower scores (Fig. 8a). W1 had lower F1 scores and a smaller range compared with the main channel sites. Groundwater sites closely clustered around an F1 score of zero while tributaries (B1–B2) and L1 tended to have negative scores (Fig. 8a).

Groundwater had consistently negative F2 scores, which created a separate cluster of data from the near zero F2 scores of tributaries B1 and B2 (Fig. 8a). The farm pond (L1) consistently had positive F2 scores that form a tight cluster separate from most other groups when plotted against F1 (Fig. 8a). Main channel water and O1 have the highest F2 ranges, with a few main channel points plotting higher than O1 (Fig. 8a). These
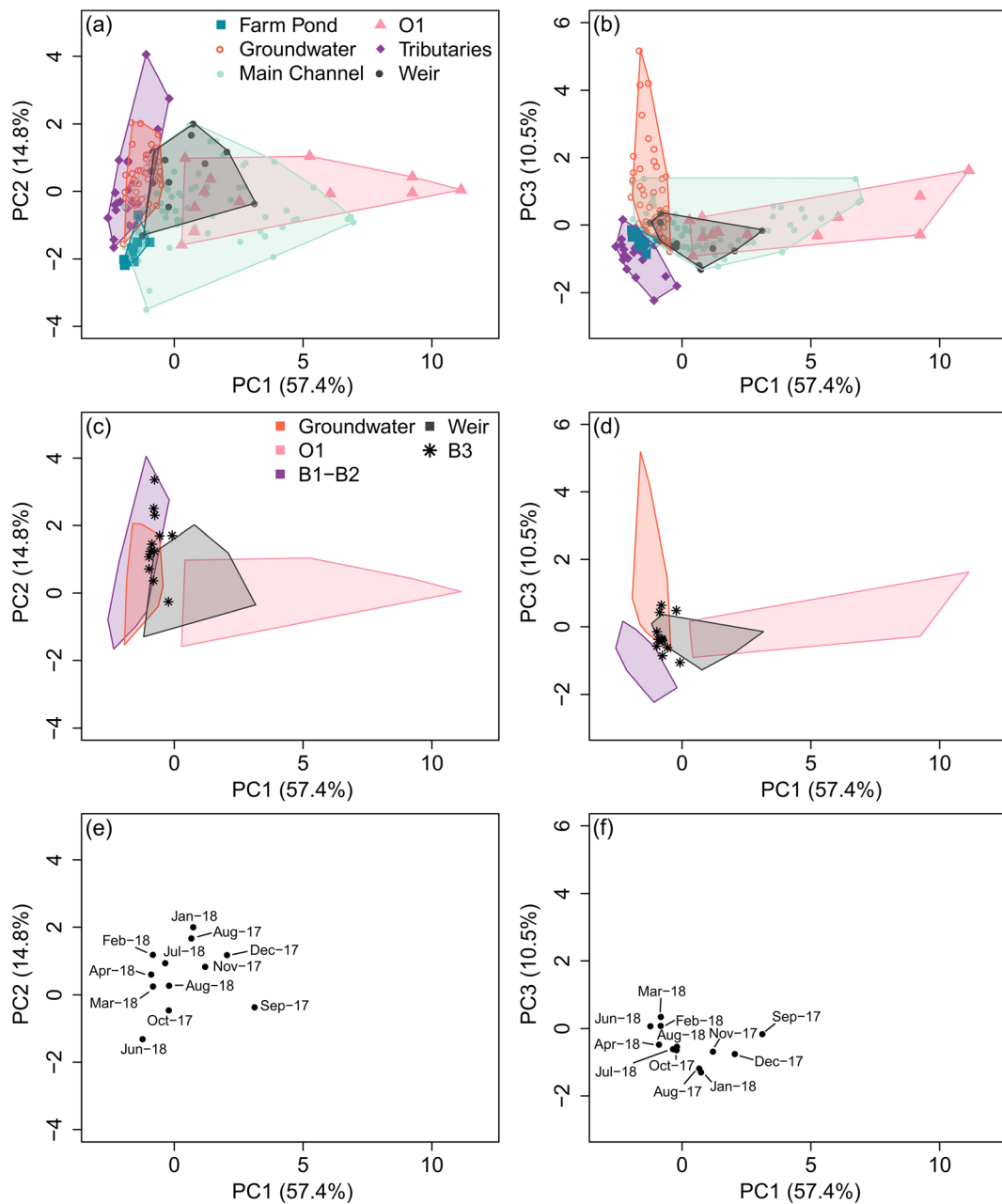
Fig. 7 (**a**) PC scores of PC1 vs PC2 for sampling stations. Stations were divided into the farm pond (L1), groundwater (SPR1, SPR2, SPR3, T1), main channel (O2, C1, C2, C3, C4, C5, C6), site O1, tributaries (B1, B2), and site W1. The range of PC scores for each group is traced in a colored polygon. (**b**) PC scores of PC1 vs PC3 for sampling stations. (**c**) Simplified polygon traces of O1, tributaries, and W1 for PC1 vs PC2 plot. Tributary B3 is plotted separately to compare the points to groundwater sites. (**d**) Simplified polygon traces of O1, tributaries, and W1 for PC1 vs PC3 plot. (**e**) W1 sample PC score labeled by sampling month for PC1 vs PC2 plot. (**f**) W1 sample PC score labeled by sampling month for PC1 vs PC3 plot

points correspond to the December 2017 data, when site O2 may have been more influential due to higher flow. F2 scores for W1 cluster between the main channel, tributary, and groundwater data ranges (Fig. 8a).

Most of the F3 scores for tributaries B1–B2 plotted in the low positive range, while groundwater sites plotted in the low negative range (Fig. 8b). When tributaries and groundwater F3 scores are plotted against F1 scores they

Table 1 Details of the factor analysis conducted in R with the nFactor package. Factors with dashes indicate no significant correlation

Factor loadings (Varimax normalized):

Variable	Factor 1	Factor 2	Factor 3
Mg^{2+}	0.954	0.131	–
Ca^{2+}	0.934	0.118	0.33
K^+	0.754	0.486	0.398
Na^+	0.671	–	–
NH_4^+	0.657	0.626	0.232
Cl^-	0.729	0.503	0.286
PO_4^{2-}	0.462	0.157	0.578
SO_4^{2-}	–	−0.255	−0.529
NO_3^-	–	−0.359	−0.122
Sum of squares loadings	3.987	1.131	1.044
Eigenvalues	5.173	1.335	0.953
Proportion of total variance	0.443	0.126	0.116
Cumulative variance	0.443	0.569	0.685

form mostly separate data clusters (Fig. 8b). O1 has the largest range of F3 scores with the highest score in September 2017 (Fig. 8b). When comparing F3 against F1 for site O1, the cluster of points overlaps the groundwater cluster during the late summer and early fall of 2018 (Fig. 8b). The main channel and W1 sites form data clusters within the O1, tributary, and groundwater data clusters (Fig. 8b).

Simplified FA plots showed near separate clusters of data for tributaries, groundwater, and O1 (Fig. 8c–d). Site W1 plots between these data clusters with most overlap occurring with O1 and groundwater data clusters (Fig. 8c–d). Tributary B3 occurs downstream from the groundwater sources of T1 and SPR2 plots mostly within the groundwater cluster as opposed to the separate cluster shown for B1 and B2 (Fig. 8c–d). W1 samples tended to have positive F1 scores in the fall and winter and negative F1 scores in spring and summer (Fig. 8e). F2 and F3 scores for W1 erratically oscillate between positive and negative values over the 12-month sampling interval without an apparent seasonal pattern (Fig. 8e–f).

PHREEQC and Piper diagrams

Averaged major ion distribution on a Piper diagram indicated that all samples plot closely as Ca^{2+}-Mg^{2+}-HCO_3^- type water (Supplemental Figure 3). When the three major groups identified by PCA and FA are plotted, main channel waters plot between them in order of upstream to downstream (Fig. 9). The O1 water plots as a marginally lower Mg^{2+} and lower SO_4^{2-} end member. Starting from O1, the channels C1–C3 plot in a straight sequential line towards the tributary end member, enriched in Mg^{2+}, Na^+, K^+, and SO_4^{2-} (Fig. 9). C4–C6 samples move in a sequential straight line towards the groundwater end member, depleted in Na^+, K^+, and SO_4^{2-} relative to tributaries (Fig. 9). There was some variation in anion distribution among the groundwater end member, although the cations plotted similarly (Fig. 9). Typically, SPR 1 and SPR 3 were enriched in SO_4^{2-} and Cl^- compared with SPR2, B3, and T1.

A simple binary and ternary mixing model between these three end members indicated that channel water patterns could be reproduced with mixing alone (Fig. 10). The proportions of each end member in the mixing models are displayed in Supplemental Table 1. Binary mixing between O1 and tributary waters reasonably simulated the pattern observed for main channel sites C1–C3. A mixture with 40% O1 water and 60% tributary water reproduces the average ion distributions of sites C3–C4. From this point, a ternary mixture of increasing groundwater end member contributions moved average sample data in the same direction as observed in Fig. 9 (Fig. 10). A mixture of about 20% O1, 50% tributary, and 30% groundwater approximates the average ion distribution of water at site C6.

Spatial analysis

Spatial analysis indicated that approximately 10% of the 4th order Muddy Creek watershed was covered by catchments similar to the study site. These catchments vary in size between 0.5 and 0.02 km^2 and were approximately evenly spaced across the entire basin (Supplemental Figure 4). The catchment in this study represents one of the larger catchments (0.5 km^2) as the median watershed size was 0.05 km^2 for the 189 catchments identified.

Comparisons of land cover between the 4th order Muddy Creek watershed and the 189 identified catchments imply potentially large impacts from agriculture and development. Both the 4th order basin and identified catchments were roughly similar overall with respect to land cover (Supplemental Figure 5). The most prevalent land cover categories were pasture, forest, and open development. Identified catchments were more
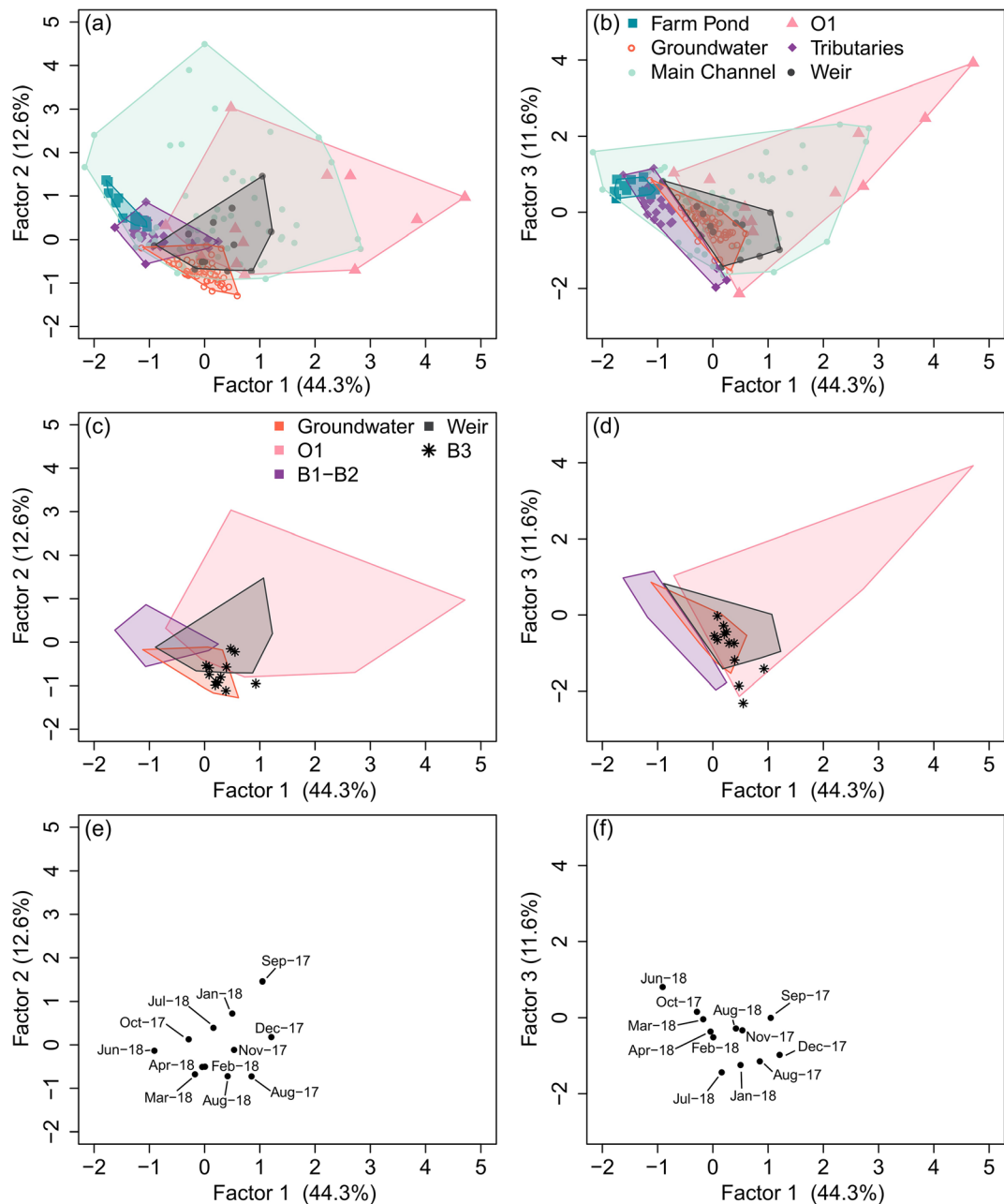
Fig. 8 (a) Factor analysis (FA) scores of F1 vs F2 for sampling stations. Stations were divided into the farm pond (L1), groundwater (SPR1, SPR2, SPR3, T1), main channel (O2, C1, C2, C3, C4, C5, C6), site O1, tributaries (B1, B2), and site W1. The range of FA scores for each group is traced in a colored polygon. (b) FA scores of F1 vs F3 for sampling stations. (c) Simplified polygon traces of O1, tributaries, groundwater, and W1 for F1 vs F2 plot. Tributary B3 is plotted separately to compare the points to groundwater sites. (d) Simplified polygon traces of O1, tributaries, groundwater, and W1 for F1 vs F3 plot. (e) W1 sample FA score labeled by sampling month for F1 vs F2 plot. (f) W1 sample FA score labeled by sampling month for F1 vs F3 plot

likely covered by cultivated crops and pasture, and less likely to have forested or developed land cover. Identified catchments were also likely to have some kind of development although most fell below 10% total land

coverage (Fig. 11a). In contrast, agricultural land cover (pasture or cultivation) in identified catchments tended to be > 50% of land coverage with most catchments exhibiting some amount of agricultural land cover (Fig.
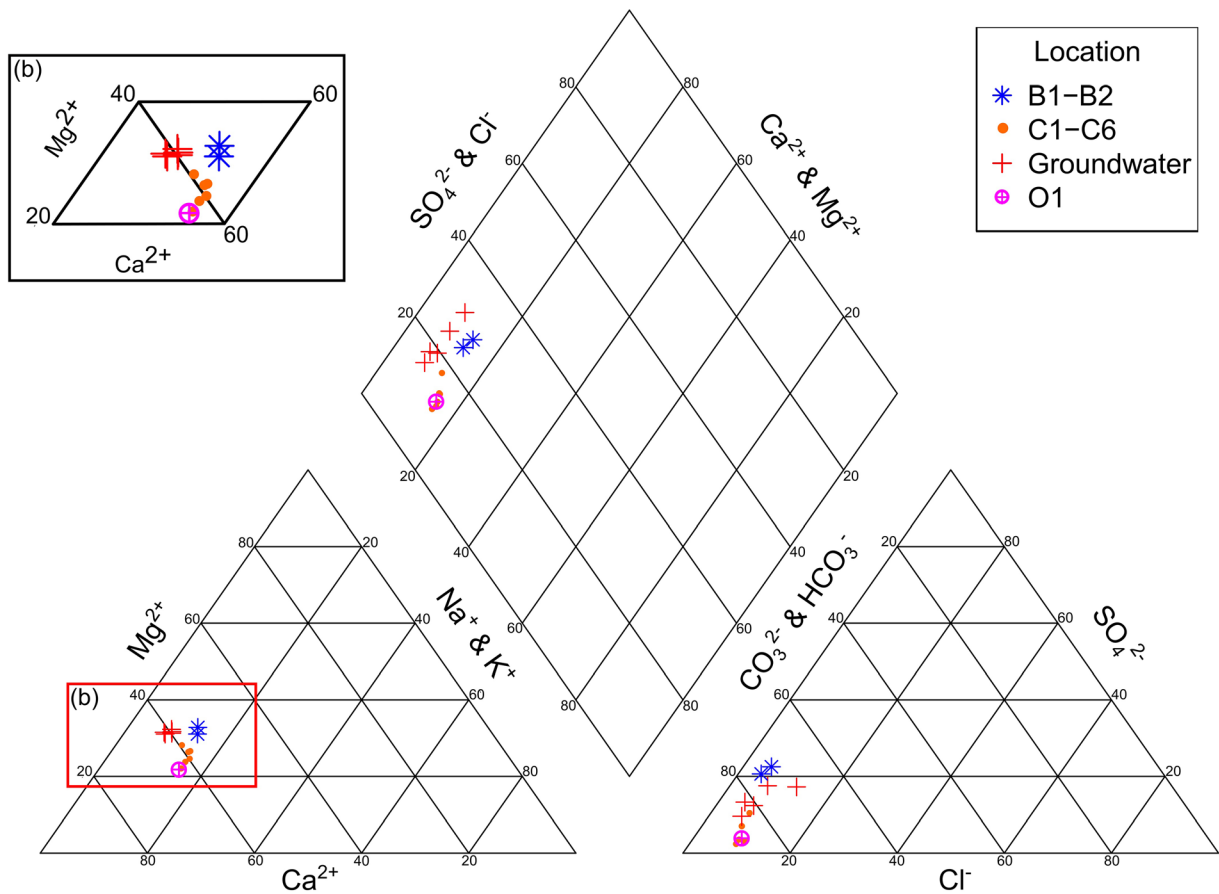
Fig. 9 Piper diagram showing the major ion percentages calculated from average concentrations of all collected data for tributaries (B1, B2), the main channel sites (C1, C2, C3, C4, C5, C6), groundwater (SPR1, SPR2, SPR3, T1, B3), and site O1. (**b**) Inset magnifying the major cations in the red box. Note the channel site values move first towards the tributary values and then towards groundwater after the confluence with B3

11b). Also, most catchments had some forested coverage, which tended to fall below 50% total coverage (Fig. 11c). Almost all of the 189 catchments contained some mixture of agricultural and forested coverage, while ~ 50% of all catchments were classified as undeveloped (Fig. 11d).

Discussion

Identification of water sources

PCA, FA, and Piper diagrams independently suggest three water sources control stream channel chemistry. PC1 and F1 both identified water sourced from the more developed portions of the study area, associated with site O1 (Figs. 6, 7, and 8, Table 1). O1 consistently had higher concentrations of salts, NH_4^+, and PO_4^{3-} skewing PC1 and F1 loadings to larger positive values (Figs. 7 and 8). C1–C6 samples exhibit successively diminishing PC1 and F1 values, reflecting dilution of O1 by downstream addition of groundwater and surface water. PC2 and F3 both identified groundwater as a SO_4^{2-}-rich source associated with springs, tributaries, and tile drains (Figs. 7 and 8). Data clusters range from unaltered groundwater (high SO_4^{2-}) to modified surface waters based on the PC1 vs PC2 plot (Fig. 7a). Tributary water overlapped the groundwater cluster, reflecting the influence of groundwater at B1 and B2 (Fig.7a). F3 also indicated an inverse relationship between SO_4^{2-} and PO_4^{3-} (Table 1). This separated groundwater from O1 and showed the gradual decline in PO_4^{3-} and increase in SO_4^{2-} in the channel waters as these two sources interact. PC3 and F2 both identified tributaries B1–B2 as
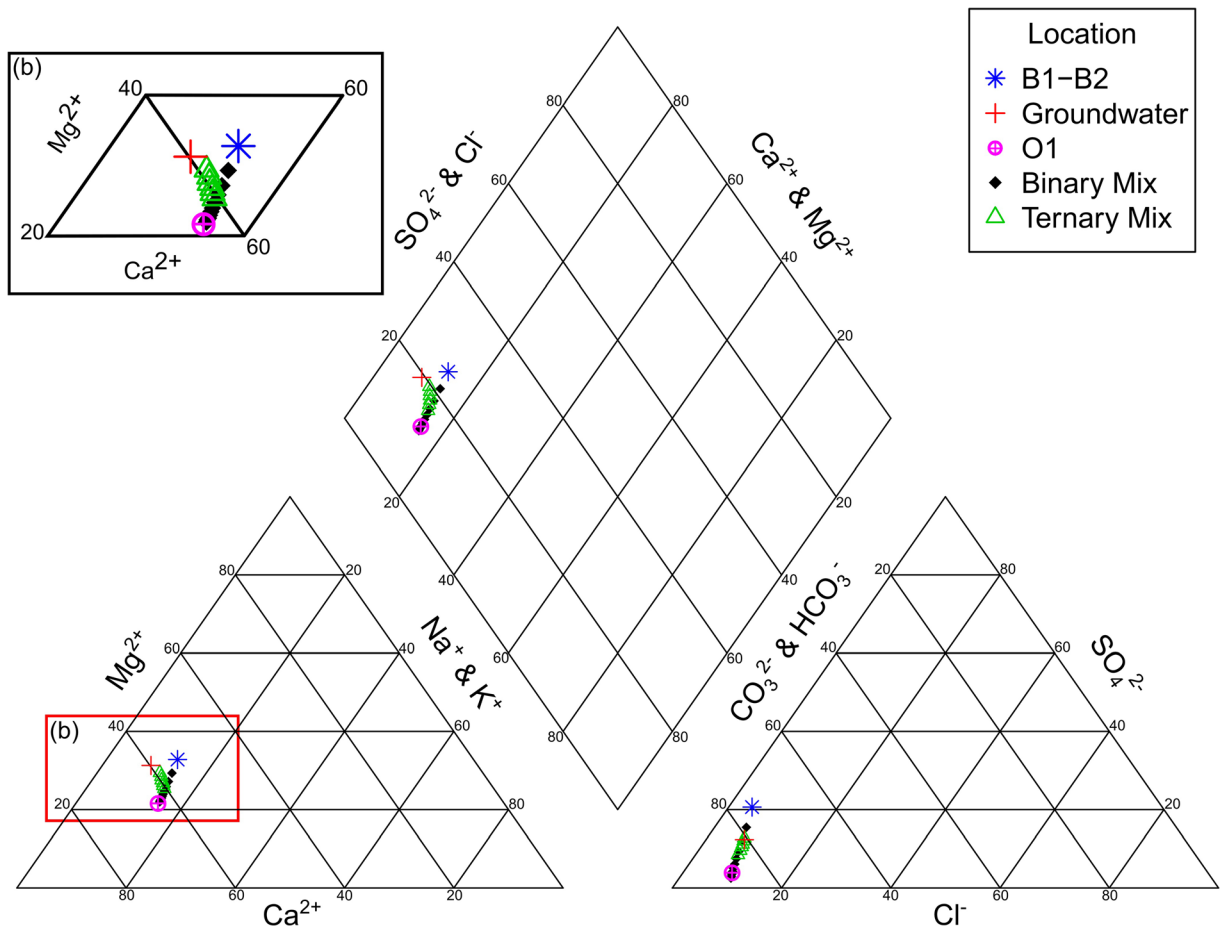
Fig. 10 Piper diagrams showing the major ion percentages of simulated mixtures between the three end members found in the catchment. The black diamonds simulate binary mixing between tributaries B1–B2 with water from O1. Green triangles simulate ternary mixing with the additional groundwater end member. (**b**) Inset magnifying the major cations in the red box. Note that ternary mixing can approximate the average channel concentration pattern found in Fig. 9

distinct from other groundwater, primarily due to lower NO_3^- concentrations (Figs. 7 and 8). Groundwater and tributaries form distinct positive and negative clusters in PC3 (Fig. 7b). Additionally, F2 shows an inverse relationship between K^+-NH_4^+-Cl^--rich water and NO_3^--rich water (Table 1). This inverse relationship differentiated B1–B2 from other groundwater due to the lower Cl^- and NO_3^- in tributary water (Fig. 8a). Moreover, Piper diagrams support PCA and FA interpretation that three source water end members control main channel water chemistry. Channel samples plot between B1–B2, groundwater, and O1 clusters, suggesting sequential ternary mixing between the three end members, which was supported by mixing models (Figs. 9 and 10). Samples from O2 and L1 were considered to have little influence on the main channel because they plot far from

the channel water and mixing models did not require their input to reproduce the average patterns. O2 may have had little influence due to much lower flow volumes relative to O1. L1 was a clay lined farm pond that may have had low connectivity with the catchment.

Base flow nutrient export

SPR1, SPR2, SPR3, T1, and B3 were considered to be representative of a groundwater end member associated with bedding plane flow. These five sites had similar Ca^{2+}, Mg^{2+}, Cl^-, SO_4^{2-}, EC, and pH, as well as relatively stable temperature ranges (Figs. 3 and 4) and tight data clusters on PC and FA plots (Figs. 7 and 8). These also plot closely together in the high Mg^{2+}-Ca^{2+}-HCO_3^- corner of the Piper diagram as expected for water in
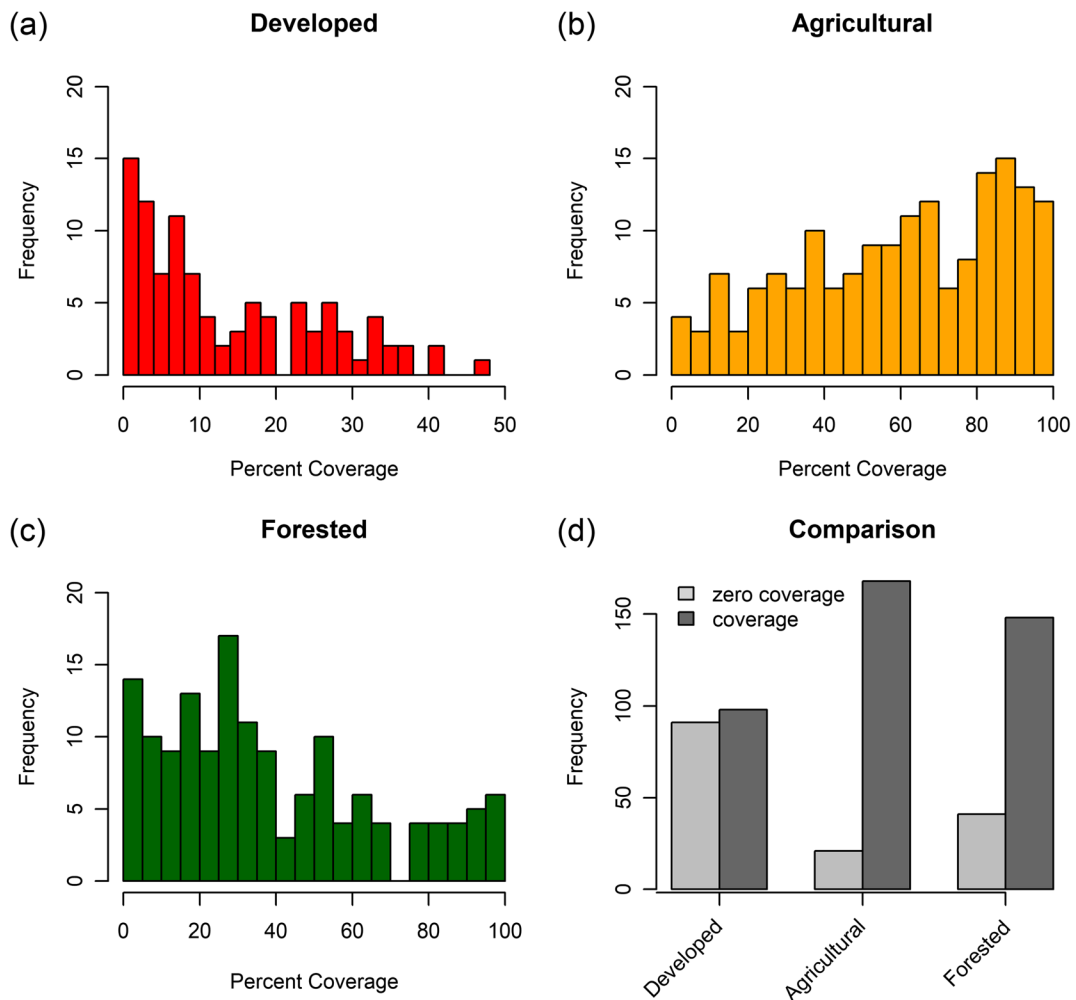
Fig. 11 (**a**) Distribution of developed land cover for identified catchments in the Muddy Creek watershed with similar characteristics to the study site. (**b**) Distribution of agricultural land cover for identified catchments. (**c**) Distribution of forested land cover for identified catchments. (**d**) Comparison of the presence or absence of land cover types in identified catchments

contact with dolomite and limestone (Fig. 9). The three springs all occur in association with the Boyle Dolomite (Supplemental Figure 1). Bedding plane flow likely controls these sites because an impermeable blue-gray clay layer outcrops in association with this unit (Supplemental Figure 2). Water moving through the area collects on top of this impermeable boundary and flows along its bedding plane until it either intersects a stream valley or emerges as a spring. We infer the controls on where a spring emerges may be related to preferential flow due to minor fractures and heterogeneity of the rock units. Support for this idea included the prevalence of thinly bedded fractured sedimentary rocks

in the region and the noted anion variation between springs. Groundwater of the study site was high in nitrate concentration as identified in PC3 and F2 (Fig. 6d, Table 1). High NO_3^- values reported in regional groundwater have been attributed to agricultural fertilizer applications (Carey et al. 1994). Local springs in the study site are likely loaded with NO_3^- from proximal agricultural infiltration collecting above the clay layer (Figs. 3h and 4h).

Tributaries B1 and B2 exhibit similar chemical compositions to groundwater, although with slightly depressed Mg^{2+}, Cl^-, NO_3^-, and EC values and higher proportions of Na^+, K^+, and SO_4^{2-} (Fig. 9). For PC1 and

PC2, the similarities in overall ion concentration and SO_4^{2-} cause the tributaries to overlap with the groundwater cluster (Fig. 7a, c). For PC3, B1 and B2 plot as a nearby, but separate cluster from groundwater, likely due to a difference in NO_3^- concentration (Fig. 7b, d). FA analysis also distinguished tributaries as similar, but produced separate clusters for both F2 and F3 due to higher relative correlations for ions such as Cl^- compared with PC2 and PC3 (Fig. 8). This suggested that these tributaries were likely sourced from and/or strongly influenced by local groundwater, which was consistent with field observations that many tributaries flowing into Muddy Creek arose from one or more springs. Because B1 and B2 are topographically higher in the research catchment, they begin in the New Albany Shale and do not cut as deeply into the Boyle Dolomite (Fig. 2, Supplemental Figure 1). Hence, B1 and B2 represent a different source water end member than springs associated with the blue-gray clay layer. The overlying New Albany Shale has a high sulfide mineral content, particularly pyrite (Nuttall 2013). Furthermore, weathering of this unit has been found to generate high SO_4^{2-} concentrations and trigger groundwater acidification in local springs due to dissolution of sulfides (Anderson 2008). Therefore, high SO_4^{2-} concentrations and lower pH of tributary samples were likely due to interaction with the New Albany Shale. B1–B2 water and groundwater likely represent a continuum between waters influenced only by the New Albany shale and waters with increasing influence from the Boyle Dolomite. This continuum probably causes lower pH at T1 compared with groundwater and generates spatial and temporal variations in spring chemistries.

Sampling site O1 was the source of the largest dissolved salt concentrations, N as NH_4^+, and P as PO_4^{3-} in the watershed channel. The O1 site converges downstream with O2 and overwhelms site C1 chemistry with the O1 chemistry signature, which persists at downstream sites (Figs. 3 and 4). Moreover, this O1 signature was attenuated downstream between C1 and C6, suggesting down-channel dilution of salts by groundwater-influenced surface water. This was supported by progressive down-channel SO_4^{2-} and NO_3^- enrichment and buffering of pH to higher values in C1–C6. As a result, water at W1 can be considered, in its simplest form, a mixture between groundwater derived from the New Albany Shale (B1–B2), groundwater derived from the Boyle Dolomite (springs), and O1 end members (Figs. 9 and 10).

Declining salt and nutrient concentrations at O1 after October 2017 (Fig. 4) can be attributed to gradual flushing of the agricultural tiles and pipeline complex (O1) that drains the developed region of the catchment. As the O1 end member contribution declines in the channel during this transition, W1 samples begin to move towards the groundwater end member along rough mixing lines observed on PCA, FA, and Piper diagrams (Figs. 7, 8, and 9). Furthermore, NO_3^- concentrations at W1 surpass those of O1 during January–March 2018, suggesting the primary source of nutrient influx during periods with less O1 influence was NO_3^--laden groundwater. Groundwater was likely receiving nitrogen from agricultural waste and fertilizer infiltration. Drainage from O1 may reflect farm operations during the growing season, discharging NH_4^+, PO_4^{3-}, and major ions, which dominate W1 nutrient output in summer. Dilution of O1 in the summer by groundwater was likely hindered by evapotranspiration and nitrate uptake (O'Driscoll and DeWalle 2010). In winter, when growing season operations and nitrogen uptake by plants cease, O1 discharge was no longer enriched with ions, so groundwater dominated the export of NO_3^- (Fig. 6). In summary, drainage from O1 exports PO_4^{3-}, NH_4^+, and other ions to W1 with less dilution from groundwater in the summer, and groundwater adds larger amounts of NO_3^- and SO_4^{2-} to dominate chemical export to W1 in winter.

The high-resolution, spatial sampling occurring monthly in this study illustrated that the developed land cover region of the farm draining through O1 seemed to control solute exports into Muddy Creek during the summer. While there was evidence of dilution from groundwater, the export of NH_4^+, Cl^-, and other ions remained elevated and additional NO_3^- was contributed to waters sampled at the outlet, W1. Aside from dilution, there was evidence that PO_4^{3-} retention occurred due to concentrations rapidly diminishing from O1–C3 without significant dilution from tributaries. During base flow, the catchment likely retained PO_4^{3-} while exporting nitrogen as NO_3^- and NH_4^+. Despite tilled fields and pasture along the channels, low concentrations of nutrients at site O2 suggested little direct transport of nutrients from these potential sources at base flow. These results are significant because they show that these small systems are sensitive to development, and nitrogen discharge from developed areas can directly enter higher order streams at elevated concentrations, especially in the case of NH_4^+. The overall impact of this

individual, small catchment on Muddy Creek water quality was likely small, but the cumulative effect of similar, multiple watersheds may combine to significantly degrade water quality in higher order streams, perhaps causing problems such as chloride toxicity and eutrophication (Causse et al. 2015; Hubbart et al. 2017).

Broader impacts

Spatial and land cover analysis imply that catchments similar to that of the study site might be significant contributors of nitrogen species to larger streams and downstream river systems. Although this study catchment was larger than most of the identified catchments in the Muddy Creek watershed, processes within these catchments are likely similar, promoting entry of NO_3^- and NH_4^+ into higher order streams. These small catchments are individually easy to dismiss because a single one accounts for less than 1% of the water volume in the main channel at base flow. However, when one considers that these catchments cover ~ 10% of this particular basin, the combined impact of their outflows becomes more significant. Moreover, these catchments are sensitive to development and agriculture, and show limited capacity to buffer water quality. In this case, the developed region of this small watershed produced the dominant geochemical signal and overall water quality was compromised, especially for dissolved nitrogen species. This shows that even a small amount of development in these types of catchments will likely have a larger than anticipated impact on water quality. Also, considering that ~ 50% of all of the 189 sub-first-order watersheds have some amount of development (Fig. 11) suggests that this may be a common process impacting water quality in the region. Because particular types or specific uses of developed areas were not distinguished, results also suggest that further research into the impact of developing sub-first-order catchments is required. Additionally, almost all of the catchments show a large amount of agricultural use, likely contributing to the degradation of water quality. The impact of agriculture observed in this research was the addition of NO_3^- to groundwater, which was released by springs under base flow conditions. These findings show that it may be possible to improve base flow water quality by controlling development in these types of catchments, while agricultural impacts may require regional scale management of groundwater resources.

Limitations

While this work shows the impact of mixing between groundwater and outfall discharge on base flow exports of nutrients in a small MLC stream, there are numerous factors to consider in continuing research. First, the monthly sampling did not include storm flows and therefore neglects well-established export processes of PO_4^{3-}, other dissolved constituents, and sediment. Storm flows generally export larger amounts of nutrients within significantly higher flow volumes. Second, further research should ideally include more conclusive chemical fingerprinting of water sources, as presence of multiple sources contributing various dissolved constituents over varied seasonal conditions makes it difficult to unambiguously pinpoint specific sources. Third, this study focused on fine-scale sampling of one small catchment, so it is important to compare these results to other such catchments to fully assess the conclusions.

Conclusion

The headwater, mixed land cover catchment in this study exhibited complex, fine-scale groundwater and surface water interactions that produced seasonal changes in nutrient and salt exports. Even small amounts of development controlled base flow nutrient levels and export of other dissolved constituents from the catchment outlet. Local groundwater dilution in the main watershed channel did not completely dilute nutrients sourced from developed regions. During the winter, NO_3^- was the dominant nutrient exported by watershed base flow and was primarily sourced from groundwater. During the growing season, NH_4^+ export from an outfall that drains developed land cover overshadowed NO_3^- export from local groundwater. These conclusions highlight that small amounts of development can have a large impact. Spatial analysis showed that catchments similar to the study site comprised 10% of the total Muddy Creek watershed, containing various levels of development that could have a significant impact on water quality. Future nutrient management strategies in this region could reduce base flow nitrogen loading of higher order streams by limiting development in small headwater catchments and regionally managing agricultural nitrogen applications that seep into groundwater.

References

Anderson, W. H. (2008). Foundation Problems and Pyrite Oxidation in the Chattanooga Shale, Estill County, Kentucky. Kentucky Geological Survey.

Appelo, C. A. J., & Postma, D. (2004). *Geochemistry, groundwater and pollution* (2nd ed.). https://doi.org/10.1201/9781439833544.

Bernal, S., Lupon, A., Ribot, M., Sabater, F., & Martí, E. (2015). Riparian and in-stream controls on nutrient concentrations and fluxes in a headwater forested stream. *Biogeosciences., 12*, 1941–1954. https://doi.org/10.5194/bg-12-1941-2015.

Brisbois, M. C., Jamieson, R., Gordon, R., Stratton, G., & Madani, A. (2008). Stream ecosystem health in rural mixed land-use watersheds. *Journal of Environmental Engineering and Science., 7*, 439–452. https://doi.org/10.1139/s08-016.

Burow, K. R., Nolan, B. T., Rupert, M. G., & Dubrovsky, N. M. (2010). Nitrate in groundwater of the United States, 1991-2003. *Environmental Science and Technology., 44*, 4988–4997. https://doi.org/10.1021/es100546y.

Burrows, R. M., Rutlidge, H., Valdez, D. G., Venarsky, M., Bond, N. R., Andersen, M. S., Fry, B., Eberhard, S. M., & Kennard, M. J. (2018). Groundwater supports intermittent-stream food webs. *Freshwater Science., 37*, 42–53. https://doi.org/10.1086/696533.

Butturini, A., Bernal, S., Nin, E., Hellin, C., Rivero, L., Sabater, S., & Sabater, F. (2003). Influences of the stream groundwater hydrology on nitrate concentration in unsaturated riparian area bounded by an intermittent Mediterranean stream. *Water Resources Research., 39,*. https://doi.org/10.1029/2001WR001260

Carey, D. I., Currens, J. C., Dinger, J. S., Kipp, J. A., Wunsch, D. R., & Conrad, P. G. (1994). Ground water in the Kentucky River Basin. *Kentucky Geological Survey Information Circular, 52*. http://www.uky.edu/KGS/pdf/ic11_52.pdf.

Causse, J., Baurès, E., Mery, Y., Jung, A. V., & Thomas, O. (2015). Variability of N export in water: a review. *Critical Reviews in Environmental Science and Technology., 45*, 2245–2281. https://doi.org/10.1080/10643389.2015.1010432.

Chen, L., Dai, Y., Zhi, X., Xie, H., & Shen, Z. (2018). Quantifying nonpoint source emissions and their water quality responses in a complex catchment: a case study of a typical urban-rural mixed catchment. *Journal of Hydrology., 559*, 110–121. https://doi.org/10.1016/j.jhydrol.2018.02.034.

Costigan, K. H., Jaeger, K. L., Goss, C. W., Fritz, K. M., & Goebel, P. C. (2016). Understanding controls on flow permanence in intermittent rivers to aid ecological research: integrating meteorology, geology and land cover. *Ecohydrology., 9*, 1141–1153. https://doi.org/10.1002/eco.1712.

Coulter, C. B., Kolka, R. K., & Thompson, J. A. (2004). Water quality in agricultural, urban, and mixed land use watersheds. *Journal of the American Water Resources Association., 40*, 1593–1601. https://doi.org/10.1111/j.1752-1688.2004.tb01608.x.

Crain, A. S., & Martin, G. R. (2009). *Concentrations, and estimated loads and yields of total nitrogen and total phosphorus at selected water-quality monitoring network stations in Kentucky, 1979–2004*. U.S. Geological Survey Scientific Investigations Report 2009–5240. Reston, Virginia.

Currens, J. C., & Graham, C. D. R. (1993). Flooding of Sinking Creek, Garretts Spring karst drainage basin, Jessamine and Woodford counties, Kentucky. *USA. Environmental Geology., 22*, 337–344. https://doi.org/10.1007/BF00767507.

Dubrovsky, N. M., Burow, K. R., Clark, G. M., Gronberg, J. A. M., Hamilton, P. A., Hitt, K. J., et al. (2010). Nutrients in the nation's streams and groundwater, 1992–2004. *US Geological Survey Circular, 1350*(2), 174.

Eaton, A. D., Clesceri, L. S., Rice, E. W., & Greenberg, A. E. (Eds.). (2005a). *Method 4500-NH3 F. Phenate method. In: Standard Methods for the Examination of Water and Wastewater* (21st ed.). APHA, AWWA, WEF. (pp. 4-153 to 4-155). Baltimore: Port City Press.

Eaton, A. D., Clesceri, L. S., Rice, E. W., & Greenberg, A. E. (Eds.). (2005b). *Method 4500-NO3 E. Cadmium reduction method. In: Standard Methods for the Examination of Water and Wastewater* (21st ed.). APHA, AWWA, WEF. (pp. 4-153 to 4-155). Baltimore: Port City Press.

Eaton, A. D., Clesceri, L. S., Rice, E. W., & Greenberg, A. E. (Eds.). (2005c). *Method 4500-P E. Ascorbic acid method. In: Standard Methods for the Examination of Water and Wastewater* (21st ed.). APHA, AWWA, WEF. (pp. 4-153 to 4-155). Baltimore: Port City Press.

English, M. (2017). hydrogeo: groundwater data presentation and interpretation. R package version 0.6-1. https://CRAN.R-project.org/package=hydrogeo. Accessed 30 Apr 2020.

Environmental Systems Research Institute [ESRI]. (2018). An overview of the Hydrology toolset. https://pro.arcgis.com/en/pro-app/tool-reference/spatial-analyst/an-overview-of-the-hydrology-tools.htm. Accessed 12 Feb 2019.

Everitt, B., & Hothorn, T. (2011). *An Introduction to Applied Multivariate Analysis with R*. New York: Springer.

Ford, W. I., King, K., & Williams, M. R. (2018). Upland and in-stream controls on baseflow nutrient dynamics in tile-drained agroecosystem watersheds. *Journal of Hydrology., 556*, 800–812. https://doi.org/10.1016/j.jhydrol.2017.12.009.

Fork, M. L., Blaszczak, J. R., Delesantro, J. M., & Heffernan, J. B. (2018). Engineered headwaters can act as sources of dissolved organic matter and nitrogen to urban stream networks.

Limnology and Oceanography Letters., 3, 215–224. https://doi.org/10.1002/lol2.10066.

Gentry, L. E., David, M. B., Royer, T. V., Mitchell, C. A., & Starks, K. M. (2007). Phosphorus transport pathways to streams in tile-drained agricultural watersheds. *Journal of Environment Quality., 36*, 408–415. https://doi.org/10.2134/jeq2006.0098.

Ghebremichael, L. T., Veith, T. L., & Hamlett, J. M. (2013). Integrated watershed- and farm-scale modeling framework for targeting critical source areas while maintaining farm economic viability. *Journal of Environmental Management., 114*, 381–394. https://doi.org/10.1016/j.jenvman.2012.10.034.

Gieskes, J. M., Gamo, T., & Brumsack, H. (1991). *Chemical methods for interstitial water analysis aboard JOIDES Resolution: College Station, Texas, Ocean Drilling Program*. ODP Tech. Note, 15(August 1991), 60.

Giri, S., Qiu, Z., Prato, T., & Luo, B. (2016). An integrated approach for targeting critical source areas to control non-point source pollution in watersheds. *Water Resources Management., 30*, 5087–5100. https://doi.org/10.1007/s11269-016-1470-z.

Gomi, T., Sidle, R. C., & Richardson, J. S. (2002). Understanding processes and downstream linkages of headwater systems: headwaters differ from downstream reaches by their close coupling to hillslope processes, more temporal and spatial variation, and their need for different means of protection from land. *BioScience, 52*(10), 905–916. https://doi.org/10.1641/0006-3568(2002)052[0905:upadlo]2.0.co;2

Greene, R. C. (1968). Geologic map of the Moberly Quadrangle, Madison and Estill Counties, Kentucky. *Kentucky Geological Survey*. https://doi.org/10.3133/gq664.

Hach. (1997). *Water Analysis Handbook* (3rd ed.). Loveland: Hach Company.

Hach. (2013). Digital Titrator Model 16900. file:///C:/Users/malzonej/Downloads/1690008_25ed(3).pdf.

Hobbie, S. E., Finlay, J. C., Janke, B. D., Nidzgorski, D. A., Millet, D. B., & Baker, L. A. (2017). Contrasting nitrogen and phosphorus budgets in urban watersheds and implications for managing urban water pollution. *Proceedings of the National Academy of Sciences., 114*, 4177–4182. https://doi.org/10.1073/pnas.1618536114.

Howarth, R. W. (2008). Coastal nitrogen pollution: a review of sources and trends globally and regionally. *Harmful Algae, 8*, 14–20. https://doi.org/10.1016/j.hal.2008.08.015.

Huang, J. J., Lin, X., Wang, J., & Wang, H. (2015). The precipitation driven correlation based mapping method (PCM) for identifying the critical source areas of non-point source pollution. *Journal of Hydrology., 524*, 100–110. https://doi.org/10.1016/j.jhydrol.2015.02.011.

Hubbart, J. A., Kellner, E., Hooper, L. W., & Zeiger, S. (2017). Quantifying loading, toxic concentrations, and systemic persistence of chloride in a contemporary mixed-land-use watershed using an experimental watershed approach. *Science of the Total Environment., 581-582*, 822–832. https://doi.org/10.1016/j.scitotenv.2017.01.019.

Husic, A., Fox, J., Agouridis, C., Currens, J., Ford, W., & Taylor, C. (2017). Sediment carbon fate in phreatic karst (Part 1): conceptual model development. *Journal of Hydrology., 549*, 179–193. https://doi.org/10.1016/j.jhydrol.2017.03.052.

Hypoxia Task Force [HTF]. (2008). Gulf Hypoxia Action Plan - 2008. Environmental Protection Agency. Retrieved from https://www.epa.gov/ms-htf/gulf-hypoxia-action-plan-2008. Accessed 16 Aug 2019.

Inamdar, S., Finger, N., Singh, S., Mitchell, M., Levia, D., Bais, H., Scott, D., & McHale, P. (2012). Dissolved organic matter (DOM) concentration and quality in a forested mid-Atlantic watershed, USA. *Biogeochemistry., 108*, 55–76. https://doi.org/10.1007/s10533-011-9572-4.

Jessen, C., Bednarz, V. N., Rix, L., Teichberg, M., & Wild, C. (2015). Marine Eutrophication. In *Environmental Indicators* (pp. 177–203). Dordrecht: Springer.

Kassambara, A. & Mundt, F. (2017). factoextra: extract and visualize the results of multivariate data analyses. R package version 1.0.5. https://CRAN.R-project.org/package=factoextra. Accessed 9 Apr 2019.

Kentucky Geography Network [KGN]. (2018). Kentucky single zone 30 ft DEM (USGS). Kentucky geography network. Commonwealth of Kentucky Environmental and Public Protection Cabinet Office of Information Services, GIS Branch. https://kygeoportal.ky.gov/geoportal/catalog/search/resource/details.page?uuid=%7B43B1D1F4-8B12-4FBB-BC8C-D9F0A911F392%7D. Accessed 25 Apr 2019.

Kentucky Geological Survey [KGS]. (2020). Kentucky geologic map information service. https://kgs.uky.edu/kgsmap/kgsgeoserver/viewer.asp. Accessed 4 Oct 2020.

Kentucky River Watershed Watch. (2010). Summary of Kentucky river watershed watch 2010 water sampling results. Kentucky Water Resources Research Institute. https://www.uky.edu/krww/sites/www.uky.edu.krww/files/2010_KRWW_summary_report_final.pdf. Accessed 10 Mar 2019.

Kentucky River Watershed Watch. (2011). Summary of Kentucky river watershed watch 2011 water sampling results. Kentucky Water Resources Research Institute. https://www.uky.edu/krww/sites/www.uky.edu.krww/files/2011_KRWW_Summary_Report.pdf. Accessed 10 Mar 2019

Kentucky River Watershed Watch. (2012). Summary report: Kentucky river watershed watch 2012 water sampling results. Kentucky Water Resources Research Institute. https://www.uky.edu/krww/sites/www.uky.edu.krww/files/2012%20KRWW%20Summary%20Report2.pdf. Accessed 10 Mar 2019.

Kentucky River Watershed Watch. (2013). A summary of the Kentucky river watershed watch 2013 water sampling results. Kentucky Water Resources Research Institute. https://www.uky.edu/krww/sites/www.uky.edu.krww/files/2013%20KRWW%20Summary%20Report%20Final.pdf. Accessed 10 Mar 2019.

Kentucky River Watershed Watch. (2014). A summary of the Kentucky river watershed watch 2014 water sampling results. Kentucky Water Resources Research Institute. https://www.uky.edu/krww/sites/www.uky.edu.krww/files/2014%20KRWW%20Summary%20Report-final.pdf. Accessed 10 Mar 2019.

Kentucky River Watershed Watch. (2015). A summary of the Kentucky river watershed watch 2015 water sampling results. Kentucky Water Resources Research Institute. https://www.uky.edu/krww/sites/www.uky.edu.krww/files/2015%20KRWW%20Summary%20Report%20Final.pdf. Accessed 10 Mar 2019.

Kentucky River Watershed Watch. (2016). A summary of the Kentucky river watershed watch 2016 water sampling results. Kentucky Water Resources Research Institute. https://www.uky.edu/krww/sites/www.uky.edu.krww/files/2016%20KRWW%20Summary%20Report_Final.pdf. Accessed 10 Mar 2019.

Kentucky River Watershed Watch. (2017). Kentucky river watershed watch summary of 2017 sampling results. Kentucky Water Resources Research Institute. https://www.uky.edu/krww/sites/www.uky.edu.krww/files/2017%20KRWW%20Summary%20Report%20Final%20Combined.pdf. Accessed 10 Mar 2019.

LaSage, D. M., Jones, A., & Edwards, T. (2006). The Muddy Creek project: evolution of a field-based research and learning collaborative. *Journal of Geoscience Education., 54*, 109–115. https://doi.org/10.5408/1089-9995-54.2.109.

Lê, S., Josse, J., & Husson, F. (2008). FactoMineR: an R Package for multivariate analysis. *Journal of Statiscal Software, 25*(1), 1–18.

Le, T. T. H., Zeunert, S., Lorenz, M., & Meon, G. (2017). Multivariate statistical assessment of a polluted river under nitrification inhibition in the tropics. *Environmental Science and Pollution Research, 24*(15), 13845–13862. https://doi.org/10.1007/s11356-017-8989-2.

Lee, D. H., Kim, J. H., Mendoza, J. A., Lee, C. H., & Kang, J. H. (2016). Characterization and source identification of pollutants in runoff from a mixed land use watershed using ordination analyses. *Environmental Science and Pollution Research., 23*, 9774–9790. https://doi.org/10.1007/s11356-016-6155-x.

Liu, C. W., Lin, K. H., & Kuo, Y. M. (2003). Application of factor analysis in the assessment of groundwater quality in a blackfoot disease area in Taiwan. *Science of the Total Environment, 313*(1–3), 77–89. https://doi.org/10.1016/S0048-9697(02)00683-6.

Loken, L. C., Crawford, J. T., Dornblaser, M. M., Striegl, R. G., Houser, J. N., Turner, P. A., & Stanley, E. H. (2018). Limited nitrate retention capacity in the Upper Mississippi River. *Environmental Research Letters., 13*. https://doi.org/10.1088/1748-9326/aacd51.

Lopez, C. B., Dortch, Q., & Jewett, E. B. (2008). *Scientific Assessment of Marine Harmful Algal Blooms.* Interagency Working Group on Harmful Algal Blooms, Hypoxia, and Human Health of the Joint Subcommittee on Ocean Science and Technology. Washington, D.C., 62.

Love, D., Hallbauer, D., Amos, A., & Hranova, R. (2004). Factor analysis as a tool in groundwater quality management: two southern African case studies. *Physics and Chemistry of the Earth., 29*, 1135–1143. https://doi.org/10.1016/j.pce.2004.09.027.

Martin-Mikle, C. J., de Beurs, K. M., Julian, J. P., & Mayer, P. M. (2015). Identifying priority sites for low impact development (LID) in a mixed-use watershed. *Landscape and Urban Planning., 140*, 29–41. https://doi.org/10.1016/j.landurbplan.2015.04.002.

McAlister, M., Akasapu, M., Albritton, B., Ormsbee, L., & Carey, D. (2010). Kentucky river watershed watch : a summary of volunteer water quality sampling efforts in the Kentucky river basin from 1999 to 2009. Kentucky Water Resources Research Institute. Retrieved from https://www.uky.edu/krww/sites/www.uky.edu.krww/files/KRWW_Ten_Year_Report_Final_Version.pdf. Accessed 10 Mar 2019.

Mehaffey, M. H., Nash, M. S., Wade, T. G., Ebert, D. W., Jones, K. B., & Rager, A. (2005). Linking land cover and water quality in New York City's water supply watersheds. *Environmental Monitoring and Assessment., 107*, 29–44. https://doi.org/10.1007/s10661-005-2018-5.

Metrohm. (2020). Manual 8.107.8050, Column manual, Metrosep C 6. https://www.metrohm.com/en/documents/81078050. Accessed 5 May 2020.

Natural Resources Conservation Service [NRCS]. (2006). Land Resource Regions and Major Land Resource Areas of the United States, the Carribean, and the Pacific Basin. United States Department of Agriculture Handbook, 296. retrieved from https://www.nrcs.usda.gov/Internet/FSE_DOCUMENTS/nrcs142p2_050898.pdf.

Nguyen, M. L., Sheath, G. W., Smith, C. M., & Cooper, A. B. (1998). Impact of cattle treading on hill land: 2. Soil physical properties and contaminant runoff. *New Zealand Journal of Agricultural Research., 41*, 279–290. https://doi.org/10.1080/00288233.1998.9513312.

Nuttall, B. C. (2013). *Middle and Late Devonian New Albany Shale in the Kentucky Geological Survey Marvin Blan No.1 Well, Hancock County, Kentucky.* Report of Investigations, Kentucky Geological Survey (Vol. 17). Kentucky Geological Survey.

O'Driscoll, M. A., & DeWalle, D. R. (2010). Seeps regulate stream nitrate concentration in a forested Appalachian catchment. *Journal of Environment Quality., 39*, 420–431. https://doi.org/10.2134/jeq2009.0083.

Olsen, R. L., Chappell, R. W., & Loftis, J. C. (2012). Water quality sample collection, data treatment and results presentation for principal components analysis - literature review and Illinois River watershed case study. *Water Research, 46*(9), 3110–3122. https://doi.org/10.1016/j.watres.2012.03.028.

Parkhurst, D. L., & Appelo, C. A. J. (2013). PHREEQC (Version 3)-a computer program for speciation, batch-reaction, one-dimensional transport, and inverse geochemical calculations. *Modeling Techniques, book 6*. Rep. 99-4259.

Pejman, A. H., Nabi Bidhendi, G. R., Karbassi, A. R., Mehrdadi, N., & Esmaeili Bidhendi, M. (2009). Evaluation of spatial and seasonal variations in surface water quality using multivariate statistical techniques. *International Journal of Environmental Science and Technology., 6*, 467–476. https://doi.org/10.1007/BF03326086.

Peterson, B. J., Wollheim, W. M., Mulholland, P. J., Webster, J. R., Meyer, J. L., Tank, J. L., et al. (2001). Control of nitrogen export from watersheds by headwater streams. *Science., 292*, 86–90. https://doi.org/10.1126/science.1056874.

Pionke, H. B., Gburek, W. J., Sharpley, A. N., & Schnabel, R. R. (1996). Flow and nutrient export patterns for an agricultural hill-land watershed. *Water Resources Research., 32*, 1795–1804. https://doi.org/10.1029/96WR00637.

Pionke, H. B., Gburek, W. J., Schnabel, R. R., Sharpley, A. N., & Elwinger, G. F. (1999). Seasonal flow, nutrient concentrations and loading patterns in stream flow draining an agricultural hill-land watershed. *Journal of Hydrology., 220*, 62–73. https://doi.org/10.1016/S0022-1694(99)00064-5.

Qiu, Z. (2009). Assessing critical source areas in watersheds for conservation buffer planning and riparian restoration.

Environmental Management., 44, 968–980. https://doi.org/10.1007/s00267-009-9380-y.

R Core Team. (2019). R: a language and environment for statistical computing. R Foundation for Statistical Computing, Vienna, Austria. https://www.R-project.org/. Accessed 6 May 2019.

Raiche, G. & Magis, D. (2020). nFactors: parallel analysis and other non graphical solutions to the Cattell Scree Test. R package version 2.4.1. https://CRAN.R-project.org/package=nFactors. Accessed 1 May 2020.

Ray, J. A., Webb, J. S., & O'dell, P. W. (1994). Groundwater sensitivity regions of Kentucky. https://kgs.uky.edu/kgsweb/download/wrs/sensitivity.pdf. Accessed 18 Feb 2019.

Royer, T. V., David, M. B., & Gentry, L. E. (2006). Timing of riverine export of nitrate and phosphorus from agricultural watersheds in Illinois: implications for reducing nutrient loading to the Mississippi River. *Environmental Science and Technology., 40*, 4126–4131. https://doi.org/10.1021/es052573n.

Shi, P., Zhang, Y., Li, Z., Li, P., & Xu, G. (2017). Influence of land use and land cover patterns on seasonal water quality at multi-spatial scales. *Catena., 151*, 182–190. https://doi.org/10.1016/j.catena.2016.12.017.

Siebers, A. R., Pettit, N. E., Skrzypek, G., Fellman, J. B., Dogramaci, S., & Grierson, P. F. (2016). Alluvial ground water influences dissolved organic matter biogeochemistry of pools within intermittent dryland streams. *Freshwater Biology., 61*, 1228–1241. https://doi.org/10.1111/fwb.12656.

Sinha, E., Michalak, A. M., & Balaji, V. (2017). Eutrophication will increase during the 21st century as a result of precipitation changes. *Science., 357*, 405–408. https://doi.org/10.1126/science.aan2409.

Strahler, A. N. (1957). Quantitative analysis of watershed geomorphology. *Eos, Transactions American Geophysical Union., 38*, 913. https://doi.org/10.1029/TR038i006p00913.

Turner, R. E., Rabalais, N. N., & Justic, D. (2006). Predicting summer hypoxia in the northern Gulf of Mexico: Riverine N, P, and Si loading. *Marine Pollution Bulletin, 52*(2), 139–148. https://doi.org/10.1016/j.marpolbul.2005.08.012.

Turner, R. E., Rabalais, N. N., & Justić, D. (2012). Predicting summer hypoxia in the northern Gulf of Mexico: Redux. *Marine Pollution Bulletin, 64*(2), 319–324. https://doi.org/10.1016/j.marpolbul.2011.11.008.

U. S. Environmental Protection Agency [EPA]. (2007). METHOD 9056A determination of inorganic anions by ion chromatography. https://www.epa.gov/sites/production/files/2015-12/documents/9056a.pdf. Accessed 24 Apr 2020.

United States Geological Survey [USGS]. (2002). High resolution national hydrography dataset (NHD) - file geodatabase extract for Kentucky. Kentucky Geography Network. https://kygeoportal.ky.gov/geoportal/catalog/search/resource/details.page?uuid=%7BAAB3592A-CCD4-4DF3-A088-3B678D69B902%7D. Accessed 21 Jan 2019.

United States Geological Survey [USGS]. (2014). NLCD 2011 Land Cover (2011 Edition, amended 2014) - National Geospatial Data Asset (NGDA) Land Use Land Cover. https://www.sciencebase.gov/catalog/item/581d050ce4b08da350d52363. Accessed 21 Jan 2019.

Vadas, P. A., Busch, D. L., Powell, J. M., & Brink, G. E. (2015). Monitoring runoff from cattle-grazed pastures for a phosphorus loss quantification tool. *Agriculture, Ecosystems and Environment., 199*, 124–131. https://doi.org/10.1016/j.agee.2014.08.026.

Valett, H. M., Morrice, J. A., Dahm, C. N., & Campana, M. E. (1996). Parent lithology, surface-groundwater exchange, and nitrate retention in headwater streams. *Limnology and Oceanography, 41*(2), 333–345. https://doi.org/10.4319/lo.1996.41.2.0333.

von Schiller, D., Bernal, S., Dahm, C. N., & Martí, E. (2017). Nutrient and Organic Matter Dynamics in Intermittent Rivers and Ephemeral Streams. In *Intermittent Rivers and Ephemeral Streams: Ecology and Management* (pp. 135–160). https://doi.org/10.1016/B978-0-12-803835-2.00006-1.

White, M. J., Storm, D. E., Busteed, P. R., Stoodley, S. H., & Phillips, S. J. (2009). Evaluating nonpoint source critical source area contributions at the watershed scale. *Journal of Environment Quality., 38*, 1654–1663. https://doi.org/10.2134/jeq2008.0375.

Withers, P. J. A., & Hodgkinson, R. A. (2009). The effect of farming practices on phosphorus transfer to a headwater stream in England. *Agriculture, Ecosystems and Environment., 131*, 347–355. https://doi.org/10.1016/j.agee.2009.02.009.

Wolock, D. M., Winter, T. C., & McMahon, G. (2004). Delineation and evaluation of hydrologic-landscape regions in the United States using geographic information system tools and multivariate statistical analyses. *Environmental Management, 34*(1), S71–S88. https://doi.org/10.1007/s00267-003-5077-9.

Wu, J., & Tanaka, K. (2016). Reducing nitrogen runoff from the Upper Mississippi River Basin to control hypoxia in the Gulf of Mexico: easements or taxes? *Marine Resource Economics, 20*, 121–144. https://doi.org/10.1086/mre.20.2.42629465.

Zimmer, M. A., & McGlynn, B. L. (2017). Bidirectional stream–groundwater flow in response to ephemeral and intermittent streamflow and groundwater seasonality. *Hydrological Processes., 31*, 3871–3880. https://doi.org/10.1002/hyp.11301.

Zimmer, M. A., & McGlynn, B. L. (2018). Lateral, vertical, and longitudinal source area connectivity drive runoff and carbon export across watershed scales. *Water Resources Research., 54*, 1576–1598. https://doi.org/10.1002/2017WR021718.